Published OnlineFirst October 26, 2016; DOI: 10.1158/2159-8290.CD-15-1263

RESEARCH ARTICLE

The Master Neural Transcription Factor BRN2 Is an Androgen Receptor–Suppressed Driver of Neuroendocrine Differentiation in Prostate Cancer

Jennifer L. Bishop[1], Daksh Thaper[1,2], Sepideh Vahid[1,2], Alastair Davies[1], Kirsi Ketola[1], Hidetoshi Kuruma[1], Randy Jama[1], Ka Mun Nip[1,2], Arkhjamil Angeles[1], Fraser Johnson[1], Alexander W. Wyatt[1,2], Ladan Fazli[1,2], Martin E. Gleave[1,2], Dong Lin[1], Mark A. Rubin[3], Colin C. Collins[1,2], Yuzhuo Wang[1,2], Himisha Beltran[3], and Amina Zoubeidi[1,2]

ABSTRACT

Mechanisms controlling the emergence of lethal neuroendocrine prostate cancer (NEPC), especially those that are consequences of treatment-induced suppression of the androgen receptor (AR), remain elusive. Using a unique model of AR pathway inhibitor–resistant prostate cancer, we identified AR-dependent control of the neural transcription factor BRN2 (encoded by *POU3F2*) as a major driver of NEPC and aggressive tumor growth, both *in vitro* and *in vivo*. Mechanistic studies showed that AR directly suppresses BRN2 transcription, which is required for NEPC, and BRN2-dependent regulation of the NEPC marker SOX2. Underscoring its inverse correlation with classic AR activity in clinical samples, BRN2 expression was highest in NEPC tumors and was significantly increased in castration-resistant prostate cancer compared with adenocarcinoma, especially in patients with low serum PSA. These data reveal a novel mechanism of AR-dependent control of NEPC and suggest that targeting BRN2 is a strategy to treat or prevent neuroendocrine differentiation in prostate tumors.

SIGNIFICANCE: Understanding the contribution of the AR to the emergence of highly lethal, drug-resistant NEPC is critical for better implementation of current standard-of-care therapies and novel drug design. Our first-in-field data underscore the consequences of potent AR inhibition in prostate tumors, revealing a novel mechanism of AR-dependent control of neuroendocrine differentiation, and uncover BRN2 as a potential therapeutic target to prevent emergence of NEPC. *Cancer Discov; 7(1); 54–71. ©2016 AACR.*

[1]Vancouver Prostate Centre, Vancouver, British Columbia, Canada. [2]Department of Urologic Sciences, Faculty of Medicine, University of British Columbia, Vancouver, British Columbia, Canada. [3]Department of Medicine, Division of Hematology and Medical Oncology, Weill Cornell Medical College, New York, New York.

Note: Supplementary data for this article are available at Cancer Discovery Online (http://cancerdiscovery.aacrjournals.org/).

Corresponding Author: Amina Zoubeidi, Vancouver Prostate Centre, 2660 Oak Street, Vancouver, BC V6H3Z6, Canada. Phone: 604-809-4947; Fax: 604-875-5654; E-mail: azoubeidi@prostatecentre.com

doi: 10.1158/2159-8290.CD-15-1263

Published OnlineFirst October 26, 2016; DOI: 10.1158/2159-8290.CD-15-1263

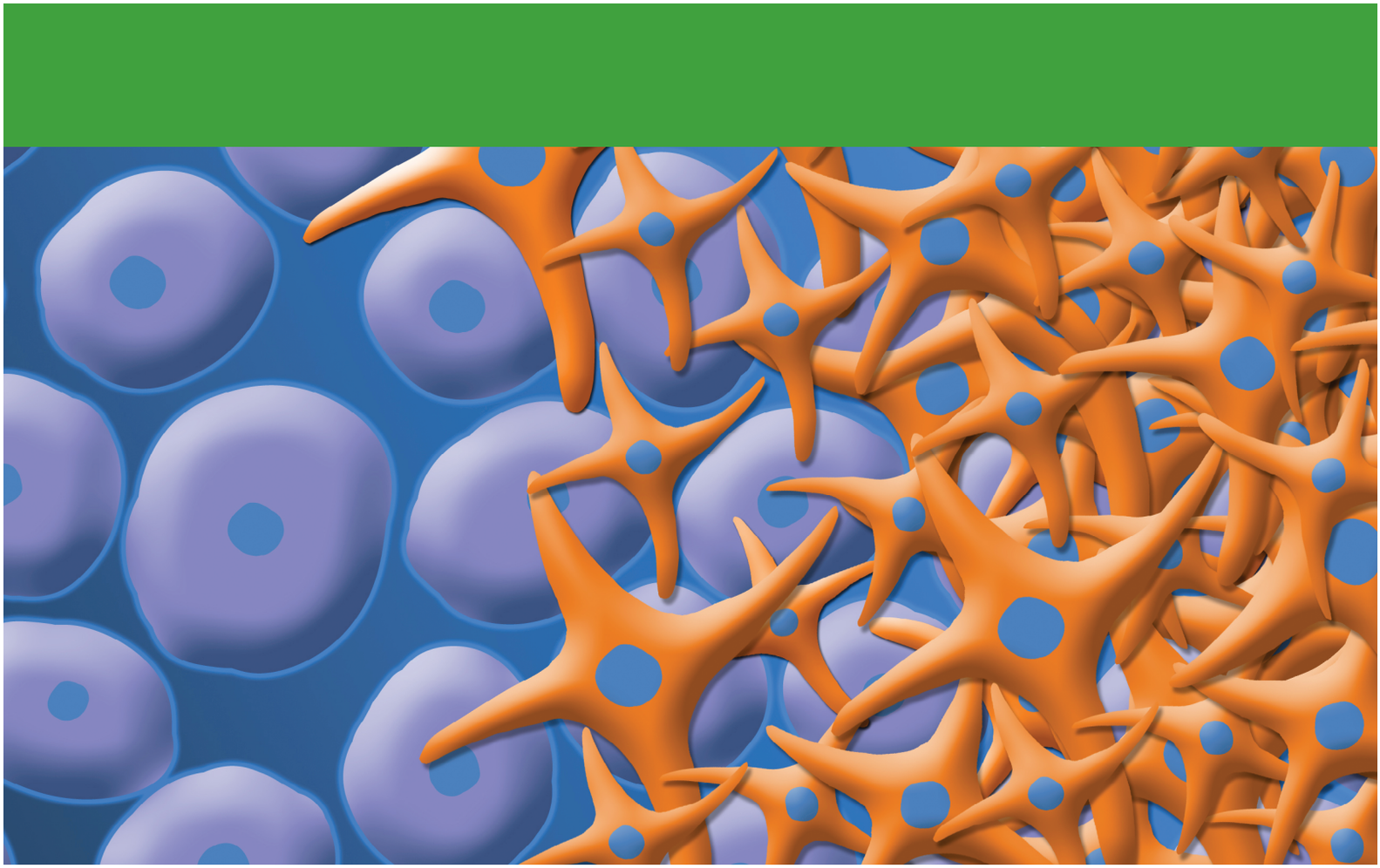

INTRODUCTION

Progression from primary prostate cancer to advanced metastatic disease is heavily dependent on the androgen receptor (AR), which fuels tumor survival. In men whose treatments for localized prostate tumors have failed, or in those who present with metastatic disease, androgen deprivation therapies (ADT) are used to deplete circulating androgens to abrogate AR signaling and prevent disease progression. Eventually, however, prostate cancer recurs after first-line ADT as castration-resistant prostate cancer (CRPC). Despite low levels of serum androgens in men with CRPC, reactivation of the AR occurs; thus, it remains central to tumor cell survival, proliferation, and metastatic spread. Targeting the AR is a cornerstone therapeutic intervention in patients with CRPC, and AR pathway inhibitors (API) that further prevent AR activation, such as enzalutamide (ENZ), have become mainstays in the prostate cancer treatment landscape (1). Despite its being a potent API, the treatment benefits of ENZ are short-lived in patients with CRPC and resistance rapidly occurs (2).

ENZ-resistant (ENZ^R) CRPC represents a significant clinical challenge not only due to the lack of third-line treatment options to prevent AR-driven tumor progression but also because it can be a precursor to rapidly progressing and lethal neuroendocrine prostate cancer (NEPC). Although NEPC can rarely arise *de novo*, it is increasingly defined as a variant of highly API-resistant CRPC (3, 4). Aside from the unique small-cell morphology and positive staining for neuroendocrine (NE) markers that characterize NEPC, it is often distinguished from prostatic adenocarcinoma by reduced AR expression or activity (5). Clinical presentation of NEPC reflects this shift away from reliance on the AR, as patients typically present with low circulating levels of PSA despite high metastatic burden in soft tissues, and are refractory to APIs (3). Importantly, it has been reported that under the strong selective pressure of potent APIs like ENZ, these "non–AR-driven" prostate cancers, which include NEPC, may constitute up to 25% of advanced, drug-resistant CRPC cases (6). Not surprisingly, therefore, the incidence of NEPC has significantly increased in recent years (7), coinciding with the widespread clinical use of APIs.

A number of molecular mechanisms likely facilitate the progression of CRPC to NEPC. These include loss of tumor suppressors, such as *RB1* (8, 9) and p53 (10), amplification of MYCN (11), mitotic deregulation through AURKA (11) and PEG10 (12), epigenetic controls such as REST (13–15) and EZH2 (11, 16), and splicing factors like SSRM4 (14, 17). Importantly, the AR plays a crucial, albeit still mechanistically unclear, role in NEPC. Reports over many years have highlighted how ADT (18, 19) or loss of AR promotes the NE differentiation of prostate cancer cells (reviewed in ref. 20); as such, many genes associated with an NE phenotype, including *ARG2* (21), *HASH1* (22), and *REST* (14, 15) are controlled by the AR. Although this evidence underscores an inverse correlation between AR expression and/or activity and molecular events leading to NEPC, the mechanisms by which the AR directly influences the induction of an NEPC phenotype

Published OnlineFirst October 26, 2016; DOI: 10.1158/2159-8290.CD-15-1263

from CRPC under the selective pressure of APIs such as ENZ remain elusive.

Answering such questions requires a model of API-resistant CRPC that recapitulates the transdifferentiation of adenocarcinoma to NEPC that occurs in patients. Herein, we present an *in vivo*–derived model of ENZ^R, which, different from others (23–25), underscores the emergence of tumors with heterogeneous mechanisms of resistance to ENZ over multiple transplanted generations. These include the natural acquisition of known AR mutations found in ENZ^R patients (25–28) and the transdifferentiation of NEPC-like tumors through an AR$^+$ state, without the manipulation of oncogenes typically used to establish NEPC in murine prostate cancer models (29–31). Using this model and data from patients with prostate cancer, we show that a master regulator of neuronal differentiation, the POU-domain transcription factor BRN2 (encoded by *POU3F2*; ref. 32), is directly transcriptionally repressed by the AR, is required for the expression of terminal NE markers and aggressive growth of ENZ^R CRPC, and is highly expressed in human NEPC and metastatic CRPC with low circulating PSA. Beyond suppressing BRN2 expression and activity, we also show that the AR inhibits BRN2 regulation of SOX2, another transcription factor associated with NEPC. These results suggest that relief of AR-mediated suppression of BRN2 is a consequence of ENZ treatment in CRPC that may facilitate the progression of NEPC, especially in men with "non–AR-driven" disease.

RESULTS

Emergence of AR-Driven and Non–AR-Driven Tumors in ENZ^R CRPC

To model ENZ^R disease, we developed cell lines from LNCaP-CRPC and ENZ^R LNCaP-CRPC xenograft tumors. LNCaP cells were used to establish subcutaneous tumors in intact male athymic nude mice and, upon tumor growth and rising PSA, mice were castrated. Once tumors recurred (CRPC), mice were treated with vehicle or 10 mg/kg ENZ daily and monitored for tumor growth (Supplementary Fig. S1A and Supplementary Methods). Although ENZ treatment did slow tumor growth compared with vehicle control, it did not prevent tumor recurrence (Fig. 1A) and the majority (9 of 10, 90%) of ENZ-treated CRPC tumors increased in tumor volume with concomitant rise in PSA (Fig. 1B). Importantly, however, PSA was not required for tumor recurrence, as observed in one mouse (Fig. 1B and C). PSA$^+$ CRPC tumors that grew in the presence of ENZ were serially transplanted into castrated male mice treated with 10 mg/kg ENZ to establish ENZ^R tumors (Supplementary Fig. S1A). Similar to the primary CRPC parental xenografts that recurred in the presence of ENZ, the majority (26 of 35, 74.3%) of transplanted tumors showed increasing volume associated with rising PSA (Supplementary Fig. S1B). However, over the course of serial transplantation, primary PSA$^+$ ENZ^R xenografts also gave rise to 9 serially transplanted tumors out of 35 (25.7%) that grew without rise in PSA (Fig. 1D–F; Supplementary Fig. S1C). Cell lines were derived from vehicle-treated CRPC (referred to as 16D^{CRPC}) and multiple transplanted ENZ^R tumors (referred to as 42D^{ENZR}, 42F^{ENZR}, 49C^{ENZR}, 49F^{ENZR}, etc.; Supplementary Fig. S1A–S1C) and were screened for protein expression of AR and PSA. Reflecting *in vivo* data, the established cell lines displayed heterogeneous expression of PSA, yet all retained expression of the AR (Fig. 1G). Importantly, 42D^{ENZR} and 42F^{ENZR} cell lines derived from PSA$^-$ tumors (Fig. 1E and Supplementary Fig. S1C and S1D) remained PSA$^-$ *in vitro* (Fig. 1G), whereas 49C^{ENZR} and 49F^{ENZR} cells derived from PSA$^+$ tumors (Fig. 1F; Supplementary Fig. S1B and S1D) retained PSA expression (Fig. 1G). Accordingly, sequencing the ligand binding domain (LBD) of the AR revealed the presence of the F878L AR activating mutation in PSA$^+$ 49C^{ENZR} and 49F^{ENZR} cells but not in PSA$^-$ 42D^{ENZR} and 42F^{ENZR} cells (Fig. 1H). Emergence of this mutation in only PSA$^+$ ENZ^R cells supports previous results showing this alteration mediates resistance to ENZ (25–28) and suggests that it may be one mechanism by which the AR is reactivated specifically in this subset of ENZ^R cells.

Mounting evidence suggests that "non–AR-driven" phenotypes of prostate cancer can emerge under the selective pressure of potent APIs like ENZ. Importantly, "non–AR-driven" tumors are not necessarily negative for AR expression; in fact, many retain AR but show reduced AR activity (33). Accordingly, our model of ENZ^R showed that approximately 25% of serially transplanted tumors, which emerged under constant presence of ENZ, may be non–AR-driven (Fig. 1D), a distribution that is echoed in clinical reports (4, 6). Indeed, RNA sequencing (Fig. 1I) and microarray analysis (Supplementary Fig. S1E) of PSA$^-$ ENZ^R cells indicated that these cells exhibited divergence in global RNA expression on principal coordinate analysis (PoCA) from either CRPC or PSA$^+$ ("AR-driven") cells and displayed reduction not only in PSA (encoded by *KLK3*) but in many classic AR-regulated genes compared with 16D^{CRPC} cells (Fig. 1J; Supplementary Fig. S1F and Supplementary Table S1). Underscoring the AR dependency of AR-driven versus non–AR-driven ENZ^R phentoypes, targeting AR using siRNA significantly reduced cell proliferation in 49F^{ENZR} cells, whereas no effect was observed in 42D^{ENZR} and 42F^{ENZR} cells (Supplementary Fig. S1F). These data suggest that emergence of ENZ resistance does not require AR reactivation and that our ENZ^R model may have utility in studying mechanisms of both classic AR-driven and non-driven disease phenotypes, especially transdifferentiation of AR$^+$ ENZ^R CRPC to NEPC.

The Neural Transcription Factor BRN2 Is Highly Expressed in NE-like ENZ^R and in Human NEPC

Our data analysis revealed that 42D^{ENZR} and 42F^{ENZR} cells exhibited reduced expression of classic AR target genes (Fig. 1J; Supplementary Fig. S1G). Additionally, 42D^{ENZR} and 42F^{ENZR} cells showed increased expression of canonical transcription factors and markers associated with neuronal development and NEPC (5), such as neuron-specific enolase (NSE), synaptophysin (SYP), chromagranin A (CGA, encoded by *CHGA*), and neural cell adhesion marker 1 (*NCAM1*; Fig. 2A; Supplementary Fig. S2A and Supplementary Table S1). The increased expression of each of these terminal NE markers was validated at the mRNA (Fig. 2B and C) and protein levels (Fig. 2D) in 42D^{ENZR} and 42F^{ENZR} cell lines and in tumors compared with CRPC controls.

Published OnlineFirst October 26, 2016; DOI: 10.1158/2159-8290.CD-15-1263

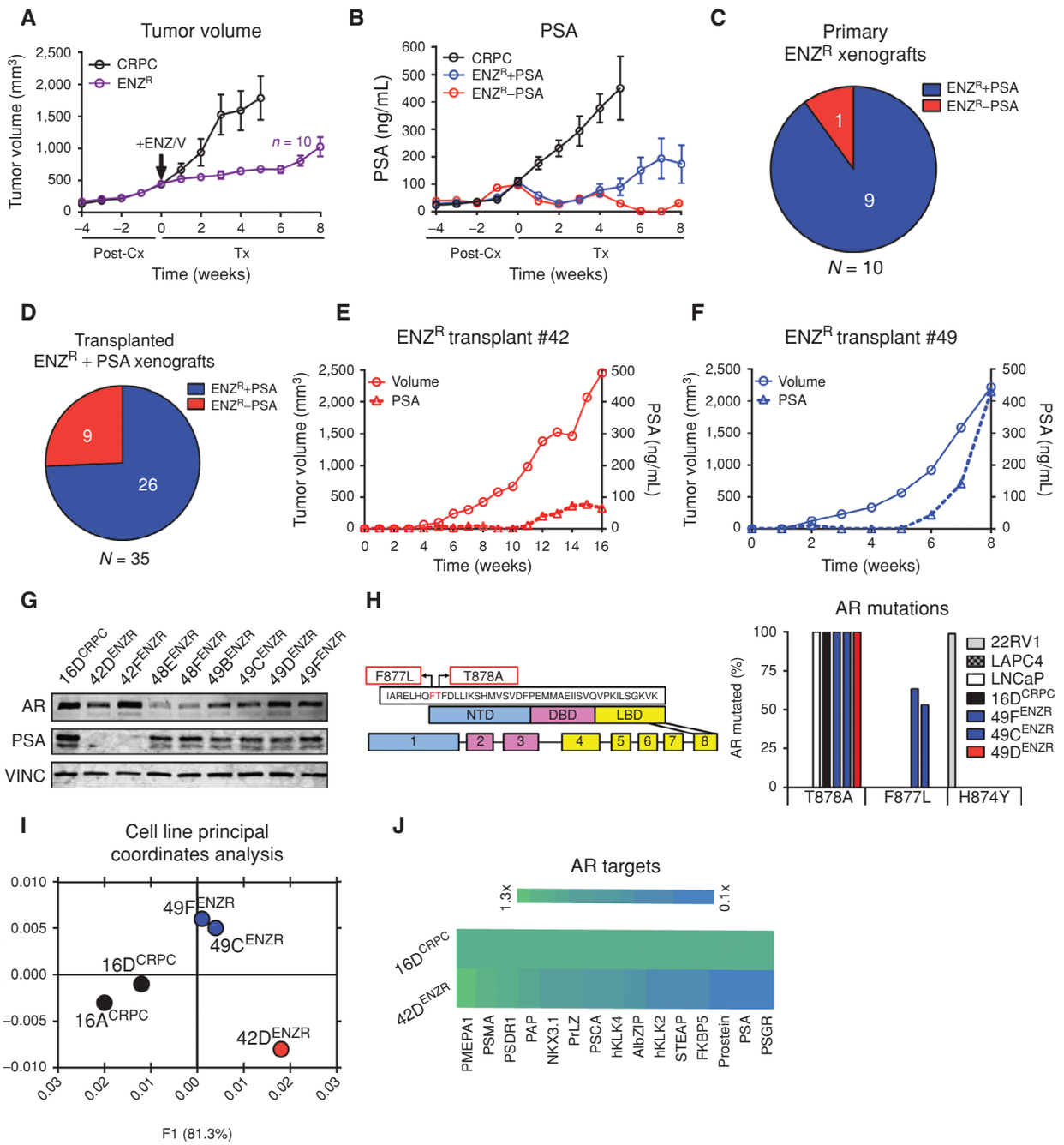

Figure 1. Emergence of AR-driven and non–AR-driven phenotypes in an *in vivo* model of ENZ^R CRPC. **A** and **B,** 1×10^6 LNCaP cells were used to establish primary and CRPC subcutaneous xenografts in male athymic nude mice. Graphs show tumor volume and corresponding serum PSA levels of tumors from 4 weeks after castration (Cx). Time 0 represents time at which serum PSA levels reached precastration levels and start of treatment (Tx) with vehicle (V, $n = 10$) or 10 mg/kg ENZ (ENZ, $n = 10$). **A,** Volumes of 10 vehicle-treated CRPC (black line) and 10 ENZ-treated (ENZ^R; purple line) tumors. **B,** Black line shows average serum PSA of vehicle-treated mice, blue line represents average serum PSA of 9 out of 10 tumors that recurred in the presence of ENZ (ENZ^R+PSA) and red line represents average serum PSA of remaining 1 tumor that recurred in the presence of ENZ (ENZ^R – PSA; $n = 10$ total, represented in purple line from **A**). **C** and **D,** Fraction of total (**C**) primary, or (**D**) transplanted, ENZ^R xenografts that recurred with (blue) or without (red) parallel rise in serum PSA (ENZ^R+/–PSA). **E** and **F,** Tumor volume and serum PSA levels for individual transplanted ENZ^R xenografts (#42 and #49) used to derive ENZ^R cell line clones 42D and 42F or 49C and 49F, respectively. **G,** Protein expression of AR, PSA, and vinculin (VINC) in CRPC and ENZ^R cell lines. **H,** Percent AR mutations in 22RV1, LAPC4, LNCaP, CRPC, and ENZ^R cell lines. **I,** Differences in global RNA expression were determined using multidimensional PoCA of RNA-sequencing data from CRPC and ENZ^R cell lines. **J,** Heat map showing fold increase in RNA-sequencing reads per million of AR target genes in 42D^{ENZR} cells compared with 16D^{CRPC} (= 1). See also Supplementary Fig. S1 and Supplementary Table S1.

Published OnlineFirst October 26, 2016; DOI: 10.1158/2159-8290.CD-15-1263

Significantly increased surface expression of NCAM1 on 42D^{ENZR} and 42F^{ENZR} cells compared with 16D^{CRPC} cells was confirmed by flow cytometry (Fig. 2E). Importantly, we found that BRN2 was strongly upregulated in our RNA sequencing data in 42D^{ENZR} versus 16D^{CRPC} cells (Fig. 2A) as well as in microarray data comparing 42F^{ENZR} versus 16D^{CRPC} cells (Supplementary Fig. S2A). Across multiple prostate cancer cell lines, BRN2 mRNA expression (Fig. 2F) was highest in the NEPC tumor–derived NCIH660 cell line and second highest in 42D^{ENZR} and 42F^{ENZR} cells. These data were reflected in serially transplanted xenografts that gave rise to 42D^{ENZR} and 42F^{ENZR} cells but not primary CRPC tumors (Supplementary Fig. S2B). These ENZ^{R} cells showed the highest BRN2 activity (Fig. 2G), and increased BRN2 expression was validated at the protein level by Western blot (Fig. 2H) and IHC (Supplementary Fig. S2C) in 42D^{ENZR} and 42F^{ENZR} cells and tumors compared with 16D^{CRPC}. In addition to NCIH660 and our ENZ^{R} cell lines, BRN2 expression was also increased in NE-like TRAMP^{+} transgenic prostate tumors (34, 35), where it positively correlated with the expression of NSE, SYP, and CGA (Fig. 2I and J). These data suggest that non–AR-driven models of ENZ^{R} display NE characteristics that may be supported by the expression of BRN2.

To investigate the clinical relevance of BRN2 in human NEPC, we assessed BRN2 expression in RNA sequencing data from prostatic hormone-naïve adenocarcinoma, CRPC, and NEPC patient tumors (Beltran cohorts; 2016, ref. 33, and 2011, ref. 11). In NEPC tumors, characterized by a high NEPC score and upregulation of canonical NE genes (Fig. 3A and B), BRN2 expression was significantly increased compared with CRPC or adenocarcinoma (Fig. 3C). Beyond this gene expression profile, NEPC is often associated with low AR activity; in these patient tumors, the AR activity score was significantly lower than adenocarcinoma or CRPC (Fig. 3D and E). Importantly, the AR score also decreased in CRPC compared with adenocarcinoma, whereas BRN2 was significantly increased (Fig. 3C and D), suggesting that BRN2 expression may be associated not only with NEPC but also with prostate cancer progression after ADT. Indeed, BRN2 expression and activity as well as NE marker expression were also increased in 16D^{CRPC} compared with parental LNCaP cells (Fig. 2F and G; Supplementary Fig. S2D), data that were in accordance with our observation in a human CRPC patient-derived xenograft (PDX) that transdifferentiated to NEPC in castrated mice (36). In this model, we found that BRN2 expression was highly upregulated in transdifferentiated NEPC versus adenocarcinoma (Fig. 3F). Increased BRN2 expression in NEPC was also observed by IHC staining (Fig. 3G and H). Importantly, IHC analysis of not only human NEPC but also CRPC and adenocarcinoma supported the inverse correlation between BRN2 and AR (Pearson R = −0.144, $P = 0.0043$) and positive correlations with CGA (Pearson R = 0.2686, $P < 0.0001$) and SYP (Pearson R = 0.2709, $P < 0.0001$). Furthermore, in patients, BRN2 was more highly expressed in metastatic CRPC than in localized adenocarcinoma (ref. 37; Supplementary Fig. S3A) and in metastatic than primary prostate cancer (ref. 38; Supplementary Fig. S3B). Finally, expression of BRN2 positively correlated with the NE-associated genes *CGA*, *CGB*, *SYP*, and *MYCN* (ref. 38; Supplementary Fig. S3C). These data show for the first time that BRN2 expression is strongly associated with severity of disease in prostate cancer, especially an NE phenotype, and that it is inversely correlated with AR activity.

BRN2 Is Inversely Correlated with AR Expression and Activity

Our observations in both NEPC patient tumors and our ENZ^{R} model led us to test the hypothesis that inhibition of the classical AR pathway increases the expression of BRN2. In accordance with our *in vitro* model where we observed PSA^{-} cell lines express BRN2, analysis of the CRPC samples in Grasso and colleagues (37) as well as the prostate adenocarcinoma data from The Cancer Genome Atlas showed an inverse correlation between BRN2 and serum PSA (Fig. 4A and Supplementary Fig. S3D). This trend was mirrored by immunohistochemistry analysis of a tissue microarray (TMA) of both CRPC specimens and treatment-naïve adenocarcinoma, where we found a significant inverse correlation between BRN2 staining intensity and circulating PSA levels in primary and CRPC patients. Moreover, BRN2 staining intensity significantly increased in progression from primary prostate cancer to CRPC only in patients with low levels of circulating PSA (Fig. 4B). *In vitro* studies further indicated that suppression of AR signaling regulates BRN2. RNA sequencing (Supplementary Fig. S4A), Western blot analysis (Supplementary Fig. S4B), and IHC (Supplementary Fig. S2C) showed that, compared with 16D^{CRPC}, the AR-driven, PSA^{+} ENZ^{R} cell lines did not upregulate BRN2 or markers of NE differentiation and showed significant reduction in BRN2 activity (Supplementary Fig. S4C). Serially transplanted tumors that gave rise to 49F cells (Supplementary Fig. S1B) were also negative for BRN2 and CGA (Supplementary Fig. S4D). Notably, in 16D^{CRPC} cells, BRN2 protein expression was increased after 2 days of

Figure 2. Non–AR-driven ENZ^{R} cells display an NE differentiation signature and increased levels of the neural transcription factor BRN2. **A,** Heat map showing fold increase in reads per million of genes involved in NE differentiation in 42D^{ENZR} cells compared with 16D^{CRPC} (= 1). **B** and **C,** Relative mRNA expression of (**B**) *NSE*, *SYP*, *CGA*, and (**C**) *NCAM1* in 42D^{ENZR} and 42F^{ENZR} cells compared with 16D^{CRPC} (= 1). **D,** Protein expression of CGA, NSE, SYP, and VINC in LNCaP, 16D^{CRPC}, 42D^{ENZR}, and 42F^{ENZR} cells and tumors. **E,** Frequency of live (7-AAD^{-}) NCAM1^{+} in LNCaP, 16D^{CRPC}, 42D^{ENZR}, and 42F^{ENZR} cells. **F,** Relative mRNA expression of BRN2 in prostate cancer (PCa) cell lines compared with LNCaP (= 1). **G,** Relative activity of luciferase under the control of BRN2 48 hours after transfection in prostate cancer cells compared with LNCaP (= 1). Luciferase (Luc) activity of BRN2 is normalized to Renilla. **H,** Protein expression of BRN2 and VINC in LNCaP, 16D^{CRPC}, 42D^{ENZR}, and 42F^{ENZR} cells (top) and LNCaP^{naïve}, 16D^{CRPC}, and 42D^{ENZR} tumors (bottom). **I,** RPKM score of BRN2 in prostate tumors or tissue isolated from TRAMP^{+} transgenic mice compared with normal. **J,** Pearson score of NSE, SYP, and CGA compared with BRN2 in TRAMP^{+} prostates. See also Supplementary Fig. S2 and Supplementary Table S1. Statistical analyses were performed on pooled data from at least three independent experiments. *, $P < 0.05$; **, $P < 0.01$; ***, $P < 0.001$; ****, $P < 0.0001$.

Published OnlineFirst October 26, 2016; DOI: 10.1158/2159-8290.CD-15-1263

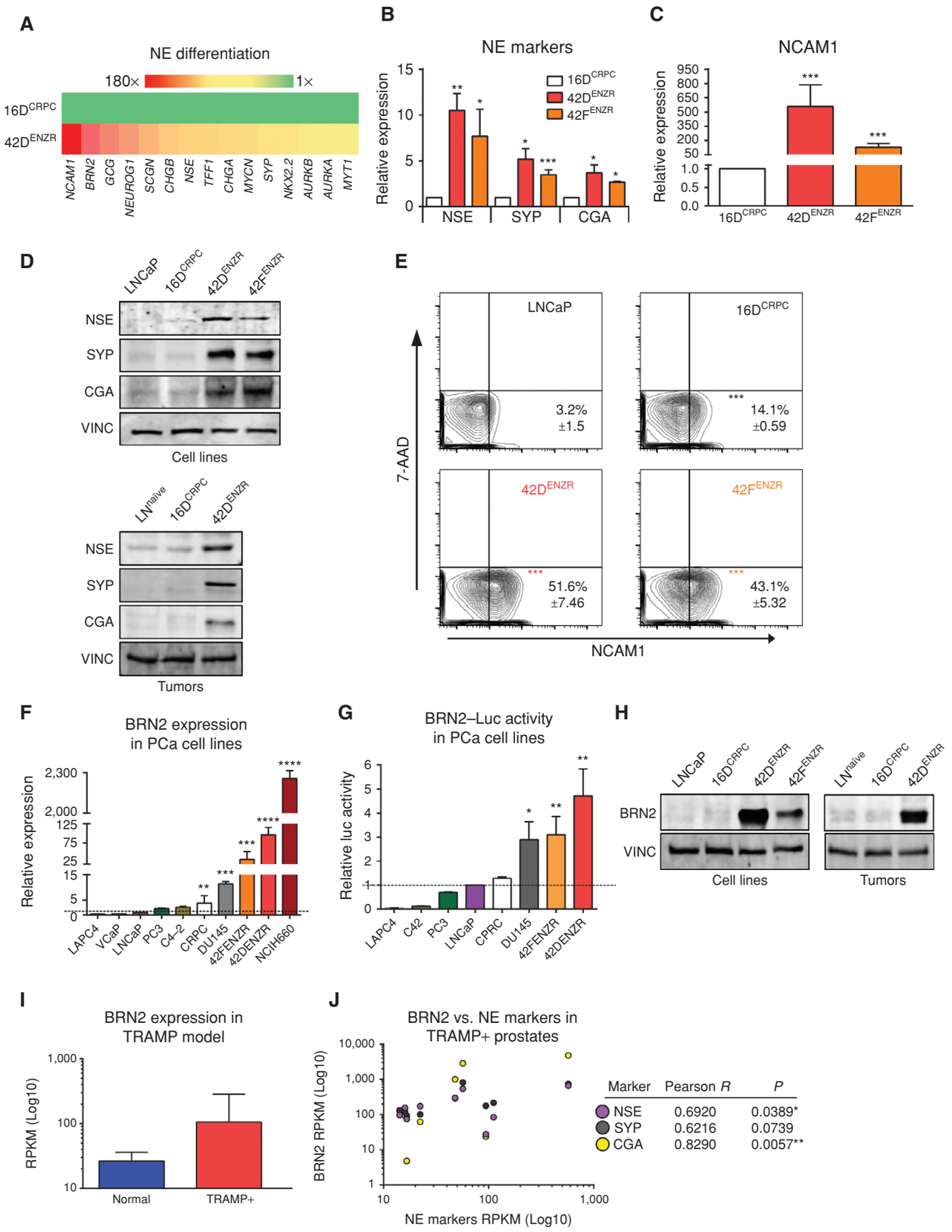

Published OnlineFirst October 26, 2016; DOI: 10.1158/2159-8290.CD-15-1263

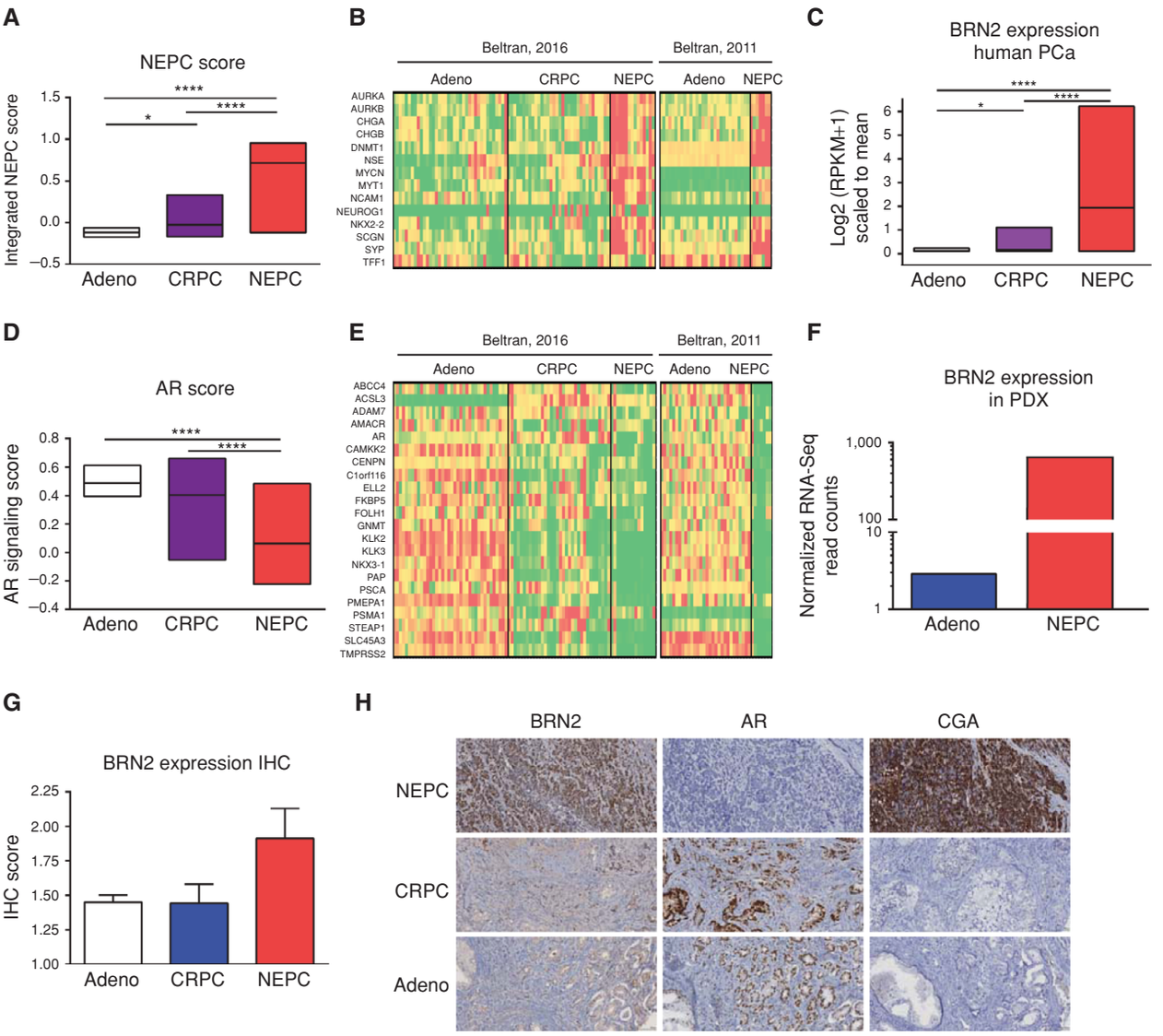

Figure 3. BRN2 is highly expressed in human NEPC. **A,** NEPC score (33); **B,** heat map of neuroendocrine associated genes, **C,** BRN2 expression (line at mean), **D,** AR score (11) and **E,** heat map of AR-regulated genes in RNA-sequencing data, obtained from two cohorts (11, 33) of Adeno ($n = 98$), CRPC ($n = 32$), and NEPC ($n = 21$) patients. **F,** BRN2 expression in patient-derived prostatic adenocarcinoma xenografts (Adeno) and terminally transdifferentiated NEPC tumors (NEPC) based on RNA sequencing. **G,** IHC score for BRN2 protein expression in adenocarcinoma (Adeno, $n = 93$), CRPC ($n = 30$), and NEPC ($n = 11$). **H,** Representative IHC for AR, BRN2, and CGA in Adeno, CRPC, and NEPC tumors. See also Supplementary Fig. S3 and Supplementary Table S2. Statistical analyses were performed on pooled data from at least three independent experiments. *, $P < 0.05$; ****, $P < 0.0001$. PCa, prostate cancer.

ENZ treatment, which was followed by increased expression of the terminal NE markers CGA, NSE, and SYP over 7 days of ENZ treatment (Fig. 4C). Importantly, siRNA-mediated silencing of *BRN2* over the course of ENZ treatment prevented the ENZ-induced upregulation of NE markers in $16D^{CRPC}$ cells (Fig. 4C) and in LAPC4 cells (Supplementary Fig. S4E). Similarly, deletion of BRN2 by CRISPR/Cas9 gene editing (Fig. 4D) or stable knockdown by shRNA (Supplementary Fig. S4F) in $16D^{CRPC}$ cells prevented ENZ-induced upregulation of NEPC markers, further confirming that BRN2 is a prerequisite for terminal NE marker expression. Reciprocally, transient overexpression of BRN2 in $16D^{CRPC}$, PC3, LAPC4, and $49F^{ENZR}$ cells was sufficient to induce expression of NSE, CGA, SYP, and NCAM1 (Supplementary Fig. S5A–S5D) and enriched for an NEPC gene signature and neuronal associated pathways in BRN2-overexpressing $16D^{CRPC}$ cells (Supplementary Fig. S5E; Supplementary Tables S2 and S3). Moreover, the effect of BRN2 overexpression on NE markers was enhanced with ENZ treatment of $16D^{CRPC}$ cells (Fig. 4E). Importantly, overexpression of BRN2 in not only $16D^{CRPC}$ cells (Fig. 4F) but also AR-driven $49F^{ENZR}$ cells (Supplementary Fig. S5F) reciprocally downregulated AR target gene expression, which was associated with significantly reduced sensitivity to ENZ in both cell lines (Fig. 4G; Supplementary

Published OnlineFirst October 26, 2016; DOI: 10.1158/2159-8290.CD-15-1263

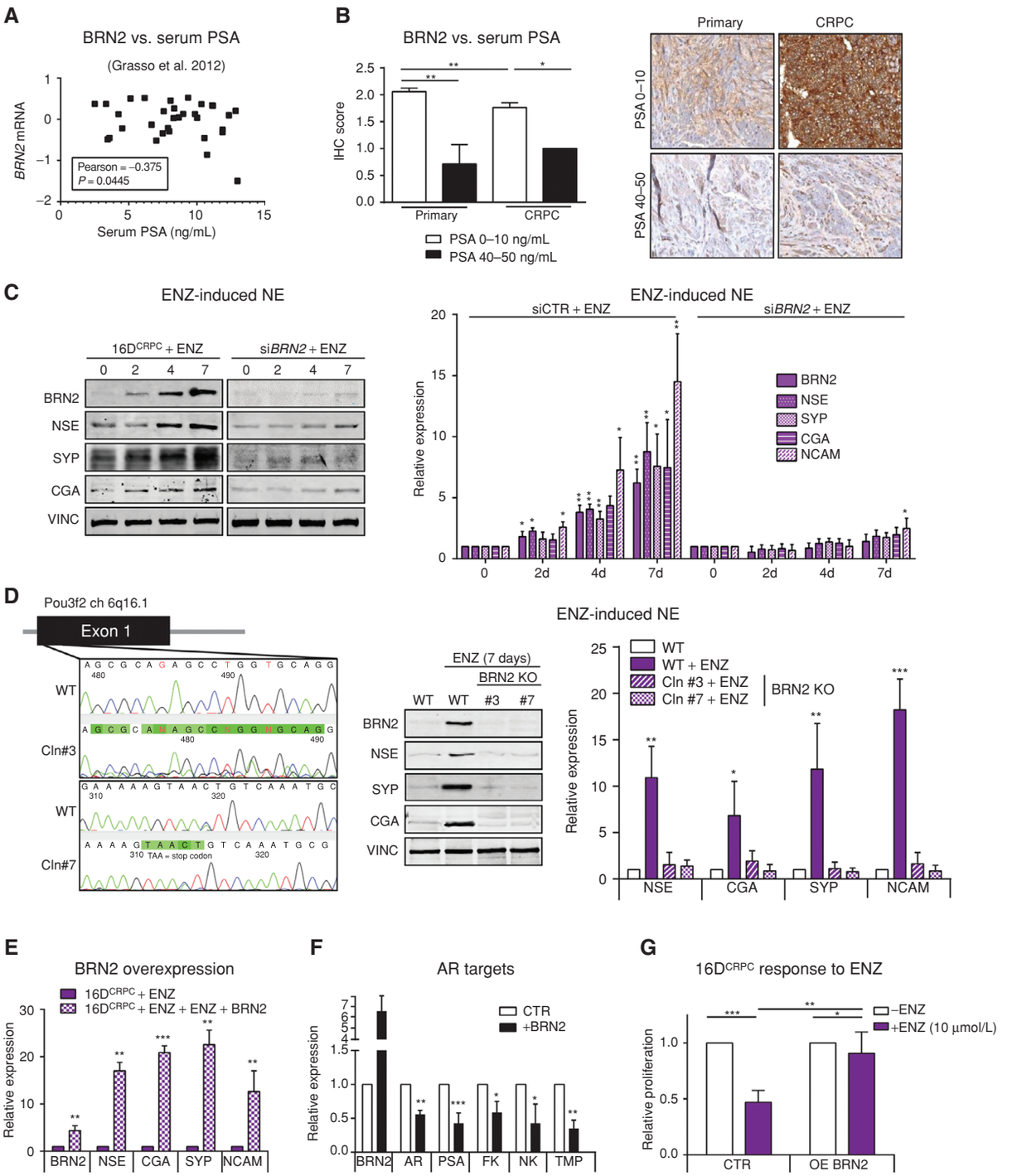

Figure 4. BRN2 expression inversely correlates with PSA in human prostate cancer and is induced by ENZ. **A,** BRN2 expression in CRPC tumors versus patient serum PSA (37). **B,** IHC score as well as representative TMA samples for BRN2 protein expression in radical prostatectomy (primary) or transurethral resection of the prostate (TURP) CRPC specimens from patients with circulating levels of PSA between 0 and 10 ng/mL or 40 and 50 ng/mL. Primary prostate cancer PSA 0–10 $n = 26$; primary prostate cancer PSA 40–50 $n = 7$; CRPC PSA 0–10 $n = 22$; CRPC PSA 40–50 $n = 2$. **C,** Protein and relative mRNA expression of BRN2, SYP, NSE, CGA, and VINC in siScr and si*BRN2* 16D^{CRPC} cells treated ± 10 μmol/L ENZ for 2, 4, or 7 days. **D,** Left, Sanger sequencing result of CRISPR/Cas9 introduction of POU3F2 deletion. The POU3F2-null clone #3 had monoallelic point mutations, whereas clone #7 had a biallelic 1-bp deletion leading to the frameshift mutation and stop codon. Mutated regions are labeled in green. **D,** Middle and right, protein and relative mRNA expression of BRN2, SYP, NSE, CGA, and VINC in different clones of 16D^{CRPC} harboring BRN2 CRISPR knockout (BRN2 KO) ± 10 μmol/L ENZ for 7 days compared with wild-type 16D^{CRPC} cells (WT). mRNA expression of BRN2 in 16D^{CRPC} WT was set to 1. **E,** Relative mRNA expression of BRN2 and NE markers in 16D^{CRPC} cells with overexpression of BRN2, treated with 10 μmol/L ENZ for 7 days compared with control vector treated (CRPC + ENZ = 1). **F** and **G,** Relative mRNA expression of AR and AR target genes in 16D^{CRPC} cells overexpressing BRN2 and (**G**) growth response of 16D^{CRPC} overexpressing BRN2 exposed to 10 μmol/L of ENZ after 72 hours. See also Supplementary Figs. S4 and S5. Statistics were performed on pooled data from at least three independent experiments. *, $P < 0.05$; **, $P < 0.01$; ***, $P < 0.001$.

Published OnlineFirst October 26, 2016; DOI: 10.1158/2159-8290.CD-15-1263

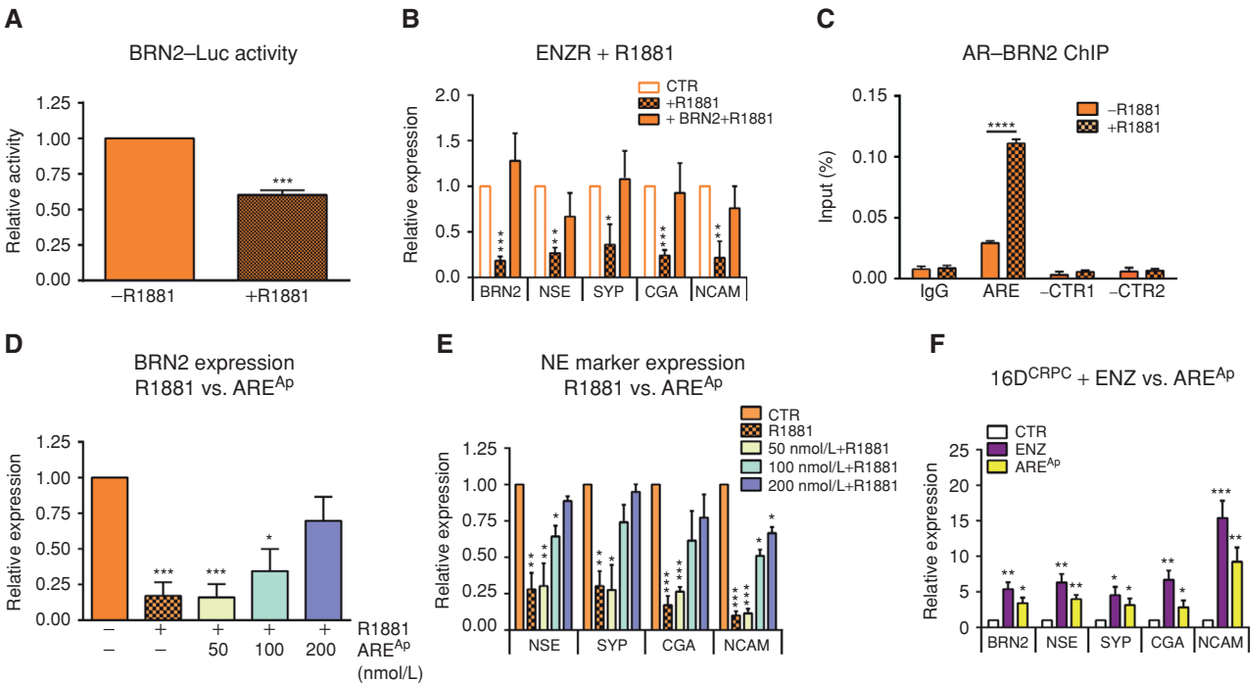

Figure 5. BRN2 activity and BRN2-dependent neuroendocrine marker expression are suppressed by AR. **A,** Relative activity of BRN2–luciferase (Luc) reporter 48 hours after transfection in 42F^{ENZR} cells treated with 10 nmol/L R1881 for 24 hours compared with control-treated cells (= 1). Luciferase activity is normalized to Renilla. **B,** Relative mRNA expression of BRN2 and NE markers in CTR transfected and 42F^{ENZR} cells overexpressing BRN2 treated with 10 nmol/L R1881 for 24 hours compared with control-treated/untransfected cells (= 1). **C,** Chromatin immunoprecipitation (ChIP) showing AR binding to the enhancer region of BRN2 in 42F^{ENZR} cells treated ±10 nmol/L R1881 for 24 hours. **D–F,** Relative mRNA expression of (**D**) BRN2 and (**E**) NE markers in 42F^{ENZR} cells treated with 10 μmol/L R1881 ± increasing doses of BRN2-ARE^{Ap} for 48 hours compared with control-treated cells (= 1) or (**F**) 16D^{CRPC} cells treated with 10 nmol/L ENZ ± increasing doses of BRN2-ARE^{Ap} for 7 days compared with control treated cells (= 1). See also Supplementary Fig. S6. Statistical analyses were performed on pooled data from at least three independent experiments. *, $P < 0.05$; **, $P < 0.01$; ***, $P < 0.001$; ****, $P < 0.0001$.

Fig. S5G). Together, these results suggest that the suppression of classic AR signaling with ENZ treatment leads to induction of an NE phenotype in CRPC that can be driven by the expression of the neural transcription factor BRN2, leading to ENZ^R.

AR Directly Represses BRN2 Expression and Activity

To address AR regulation of BRN2 in CRPC, we assessed the effects of synthetic androgen (R1881) stimulation of AR on BRN2 activity and expression. We found that R1881 significantly reduced BRN2 reporter activity in 42F^{ENZR} (Fig. 5A), 42D^{ENZR} (Supplementary Fig. S6A), and in 16D^{CRPC} cells treated with ENZ (Supplementary Fig. S6B). The expression of BRN2 mRNA was also reduced by R1881 in multiple cell lines (Fig. 5B; Supplementary Fig. S6C–S6E) and was accompanied by a reduction in terminal NE markers (Fig. 5B; Supplementary Fig. S6C and S6D). Importantly, the R1881-dependent reduced expression of NE markers was rescued by BRN2 overexpression, suggesting that it is an important upstream androgen-regulated transcription factor responsible for NE marker expression (Fig. 5B; Supplementary Fig. S6C and S6D). Indeed, we identified an androgen response element (ARE) 8,733 bp upstream of the BRN2 transcriptional start site, and chromatin immunoprecipitation (ChIP) showed that stimulation with R1881 significantly increased AR occupancy at this ARE compared with androgen-deprived conditions (Fig. 5C). To address the effect of AR binding specifically to BRN2 at this ARE, a 20-bp DNA aptamer, which physically inhibits binding of other molecules to its complementary sequence (39), was designed to prevent AR binding at the ARE in the BRN2 enhancer region, and the effects of R1881 on BRN2 and NE marker expression were assessed. The reduction of BRN2 (Fig. 5D) and NE marker (Fig. 5E) expression by R1881 treatment in ENZ^R cells could be rescued in a dose-dependent fashion by introduction of the BRN2 ARE aptamer (ARE^{Ap}). No effects of aptamer treatment were seen on other AR-dependent genes such as *PSA*, *FKBP5*, and *TMPRSS2*, indicating the specific effects of aptamer treatment on AR binding to BRN2 (Supplementary Fig. S6F). In addition, treatment of 16D^{CRPC} cells with the BRN2 ARE^{Ap} increased expression of BRN2 and NE markers to similar levels as ENZ (Fig. 5F). Taken together, these results indicate that BRN2 is negatively regulated by AR activation in both ENZ^R cells and 16D^{CRPC} cells under the pressure of ENZ.

BRN2 and AR Regulate SOX2 in NE Differentiation

As in neural development, multiple transcription factors may enhance an NE phenotype in prostate cancer. One

Published OnlineFirst October 26, 2016; DOI: 10.1158/2159-8290.CD-15-1263

candidate that has been implicated in human NEPC (40) and cooperates with BRN2 in neural cells (41) is SOX2. Indeed, SOX2 was significantly upregulated in human NEPC compared with adenocarcinoma or CRPC (Fig. 6A) as well as in our NEPC PDX (Fig. 6B) and was positively correlated with BRN2 expression in metastatic prostate cancer (ref. 37; Supplementary Fig. S7A). Like BRN2, SOX2 expression was highly expressed in NCIH660 cells, as well as in 42D^{ENZR} and 42F^{ENZR} cells compared with other prostate cancer lines (Fig. 6C). In addition, genes co-bound and co-regulated by both BRN2 and SOX2 identified in neural progenitor cells (NPC; ref. 42) were also enriched in patients with NEPC (Fig. 6D, left) and in 42D^{ENZR} and 42F^{ENZR} compared with 16D^{CRPC} cells (Fig. 6D, right; Supplementary Fig. S7B). Coregulation of these genes may be mediated by BRN2–SOX2 protein–protein interaction, which we confirmed by coimmunoprecipitation of BRN2 and SOX2 in 42D^{ENZR} and 42F^{ENZR} cells (Fig. 6E), and Re-ChIP experiments showing BRN2 and SOX2 co-occupy enhancer regions of NES and RFX4 in 42D^{ENZR} (Fig. 6F). These results showed that BRN2 and SOX2 can physically interact in prostate cancer cells and supported further investigation into the hypothesis that these two transcription factors may work in concert to promote NEPC.

Similar to BRN2, SOX2 is also negatively regulated by the AR (43). Consistently, we found that SOX2 expression was induced by ENZ treatment in 16D^{CRPC} and LAPC4 cells (Supplementary Fig. S7C), whereas R1881 reduced SOX2 expression (Supplementary Fig. S7D). Beyond the AR, however, it remains unclear what regulates SOX2 expression in prostate cancer and whether BRN2 is involved. We found that *SOX2* mRNA levels were reduced after BRN2 knockdown in ENZ^{R} (Fig. 6G), PC3, NCIH660, and ENZ-treated LAPC4 cells (Supplementary Fig. S7E–S7G), whereas overexpression of BRN2 in 16D^{CRPC} (Fig. 6H), PC3, LAPC4, or 49F^{ENZR} cells (Supplementary Fig. S7H) markedly increased *SOX2*, data that are in accordance with previous studies showing that BRN2 is required for SOX2 activity in neural development (44). Moreover, R1881-dependent suppression of *SOX2* could be rescued in ENZ^{R} cells by the addition of our BRN2 ARE aptamer (Supplementary Fig. S7I), further supporting our data that BRN2 is AR-suppressed and regulates *SOX2* expression. To investigate whether SOX2 may reciprocally regulate BRN2, we examined the enhancer region of BRN2 for potential SOX binding sites. Strikingly, we found a canonical SOX binding motif (42) that overlapped with the ARE in BRN2 (Fig. 6I, diagram). ChIP was used to validate binding of SOX2 to the same region as the AR upstream of BRN2 in ENZ^{R} cells in androgen-deprived versus stimulated conditions, and we found that SOX2 was able to bind this site in the absence, but not in the presence, of R1881 (Fig. 6I). Interestingly, however, we found that neither knockdown nor overexpression of SOX2 altered mRNA expression of BRN2 in ENZ-treated 16D^{CRPC} cells (Fig. 6J and K) or NCIH660-, PC3-, or ENZ-treated LAPC4 cells (Supplementary Fig. S7J–S7L). These results suggest a unidirectional regulation of SOX2 by BRN2 and not vice versa, and show that SOX2 binding to the BRN2 enhancer is regulated by AR.

These results strongly implicated BRN2 over SOX2 in driving an NE phenotype in CRPC cells. To investigate this hypothesis, we altered BRN2 and/or SOX2 expression with siRNA or by overexpression in multiple prostate cancer cell lines and found that although BRN2 knockdown reduced the expression of NE markers, SOX2 knockdown did not (Fig. 6J; Supplementary Fig. S7J). Reciprocally, forced expression of SOX2 marginally increased expression of terminal markers of NE differentiation in ENZ-treated 16D^{CRPC} and PC3 cells (Fig. 6K; Supplementary Fig. S7K), although not to the same extent as overexpression of BRN2 (Fig. 4E; Supplementary Fig. S5B), and did not increase NE markers in ENZ-treated LAPC4 cells (Supplementary Fig. S7L). Finally, in 16D^{CRPC} and LAPC4 cells where we simultaneously silenced BRN2 and overexpressed SOX2, we did not observe an increase in NE marker expression (Fig. 6L; Supplementary Fig. S7L), indicating that BRN2 is required for any SOX2-dependent induction of NE differentiation. Taken together, these data show, for the first time, that BRN2-dependent control of SOX2 in prostate cancer is inhibited by the AR and drives the expression of terminal NE markers. Moreover, they underscore the central role for BRN2 as a primary regulator of NEPC differentiation in prostate cancer.

BRN2 Is Required for NE Marker Expression and Aggressive Growth of ENZ^{R} Cells *In Vitro* and *In Vivo*

Our data suggested that BRN2 contributes to ENZ resistance and is a master regulator of ENZ-induced NE differentiation in CRPC. Confirming the requirement for BRN2 in supporting an NE phenotype across multiple cell lines, we found that transient targeting of BRN2 yielded a marked reduction in mRNA levels of *NSE*, *SYP*, *CGA*, and *NCAM1* in NCIH660 (Fig. 7A), 42D^{ENZR}, 42F^{ENZR}, PC3, and LAPC4 cells (Supplementary Fig. S8A–S8D). Similar results were observed in stable sh*BRN2* knockdown 42F^{ENZR} cells (Fig. 7B). In addition to the expression of terminal NE markers, we questioned whether BRN2 may be important in regulating the aggressive biology of NEPC. Therefore, we investigated the effects of BRN2 knockdown on cellular proliferation, migration, and invasion *in vitro*. BRN2 knockdown significantly reduced proliferation in both si*BRN2* NCIH660 cells and sh*BRN2* 42F^{ENZR} cells (Fig. 7C and D) and prevented wound closure in a one-dimensional scratch assay (Fig. 7E), as well as the capacity of sh*BRN2* 42F^{ENZR} cells compared with sh-control cells to migrate through a Matrigel-coated Boyden chamber (Fig. 7F). Similar results were observed in sh*BRN2* 16D^{CRPC} cells (Supplementary Fig. S8E–S8G). The reduced proliferative capacity of sh*BRN2* cells *in vitro* was translated *in vivo*; sh*BRN2* 42F^{ENZR} subcutaneous tumors grown in castrated mice under the pressure of ENZ were smaller than sh-control tumors (Fig. 7G), and these tumors had reduced expression of BRN2 and terminal NE markers (Fig. 7H), indicating that this NEPC signature was associated with more aggressive growth. These *in vitro* and *in vivo* results indicate that ENZ-induced NE differentiation is mediated by BRN2, which can be targeted to reduce invasiveness and tumor proliferation in both ENZ^{R} and CRPC.

Published OnlineFirst October 26, 2016; DOI: 10.1158/2159-8290.CD-15-1263

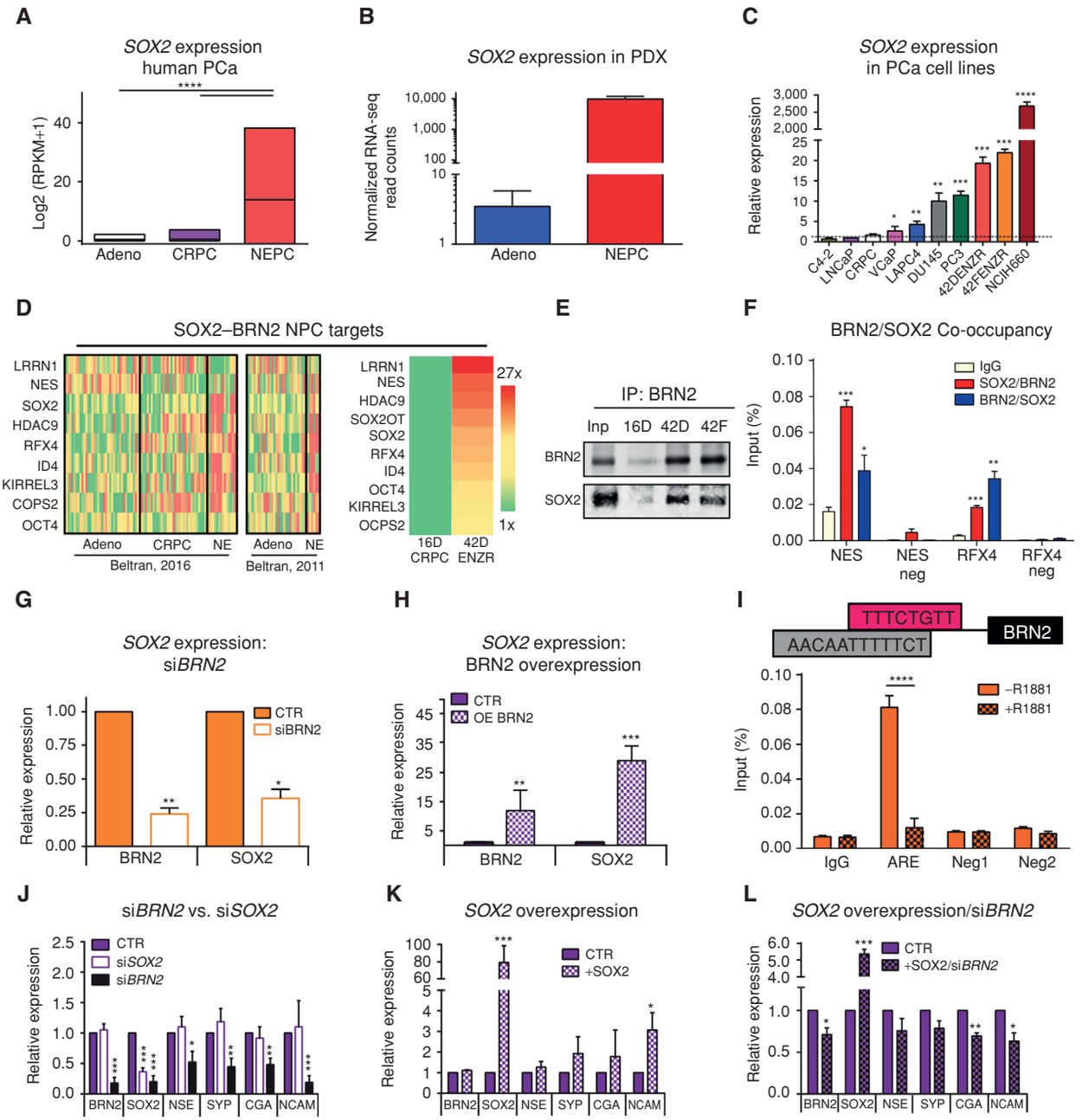

Figure 6. BRN2-dependent regulation of *SOX2* expression is inhibited by the AR and drives NE differentiation. **A,** *SOX2* expression in human prostatic adenocarcinoma (Adeno, $n = 68$), CRPC ($n = 32$), and NEPC tumors ($n = 21$; refs. 11, 33; line at mean). **B,** *SOX2* expression in patient-derived prostatic adenocarcinoma xenografts (Adeno) and terminally transdifferentiated NEPC tumors (NEPC) based on RNA sequencing (RNA-seq). **C,** Relative mRNA expression of *SOX2* across different prostate cancer cell lines compared with LNCaP as control (= 1). **D,** Left, heat map of SOX2–BRN2 co-bound neural progenitor cell (NPC) gene targets (42) in NEPC, Adeno, and CRPC tumors in two cohorts (11, 33). **D,** Right, heat map of fold increase in reads per million of genes identified as co-bound by SOX2 and BRN2 in NPCs (42) in $42D^{ENZR}$ cells compared with $16D^{CRPC}$ (= 1). **E,** SOX2–BRN2 protein interaction shown by immunoprecipitation of BRN2 and Western blot for SOX2 in $16D^{CRPC}$, $42D^{ENZR}$, and $42F^{ENZR}$ cells. **F,** Quantitative Re-ChIP analysis for the enhancer region of NES and RFX4 in $42D^{ENZR}$ cells using anti-BRN2 and anti-SOX2 antibodies with indicated sequential order (BRN2/SOX2, blue; or SOX2/BRN2, red). IgG was used as antibody control, and sequences outside of the enhancer regions were designed for the specificity of the binding. **G,** Relative mRNA expression of BRN2 and SOX2 in $42F^{ENZR}$ transfected with si*BRN2* compared with siCTR transfected cells (= 1). **H,** Relative mRNA expression of BRN2 and *SOX2* in $16D^{CRPC}$ cells overexpressing BRN2 (OE BRN2) compared with control vector (CTR = 1). **I,** Chromatin immunoprecipitation showing SOX2 binding to the enhancer region of BRN2 in $42F^{ENZR}$ cells treated with 10 nmol/L R1881 for 24 hours compared with control-treated cells (= 1). **J–L,** Relative mRNA expression of BRN2, *SOX2*, and NE markers in $16D^{CRPC}$ cells transfected with (**J**) si*SOX2*, si*BRN2*, or siCTR; **K,** SOX2 overexpression vector (OE *SOX2*) or CTR vector; **L,** *SOX2* overexpression vector + si*BRN2* (OE SOX2/si*BRN2*) or CTR vector. Post-transfection, $16D^{CRPC}$ cells were cultured in the presence of 10 μmol/L ENZ and harvested 5 days later for analysis. For each panel, relative mRNA values are compared with CTR = 1. See also Supplementary Fig. S7. Statistical analyses were performed on pooled data from at least three independent experiments. *, $P < 0.05$; **, $P < 0.01$; ***, $P < 0.001$; ****, $P < 0.0001$. PCa, prostate cancer.

Published OnlineFirst October 26, 2016; DOI: 10.1158/2159-8290.CD-15-1263

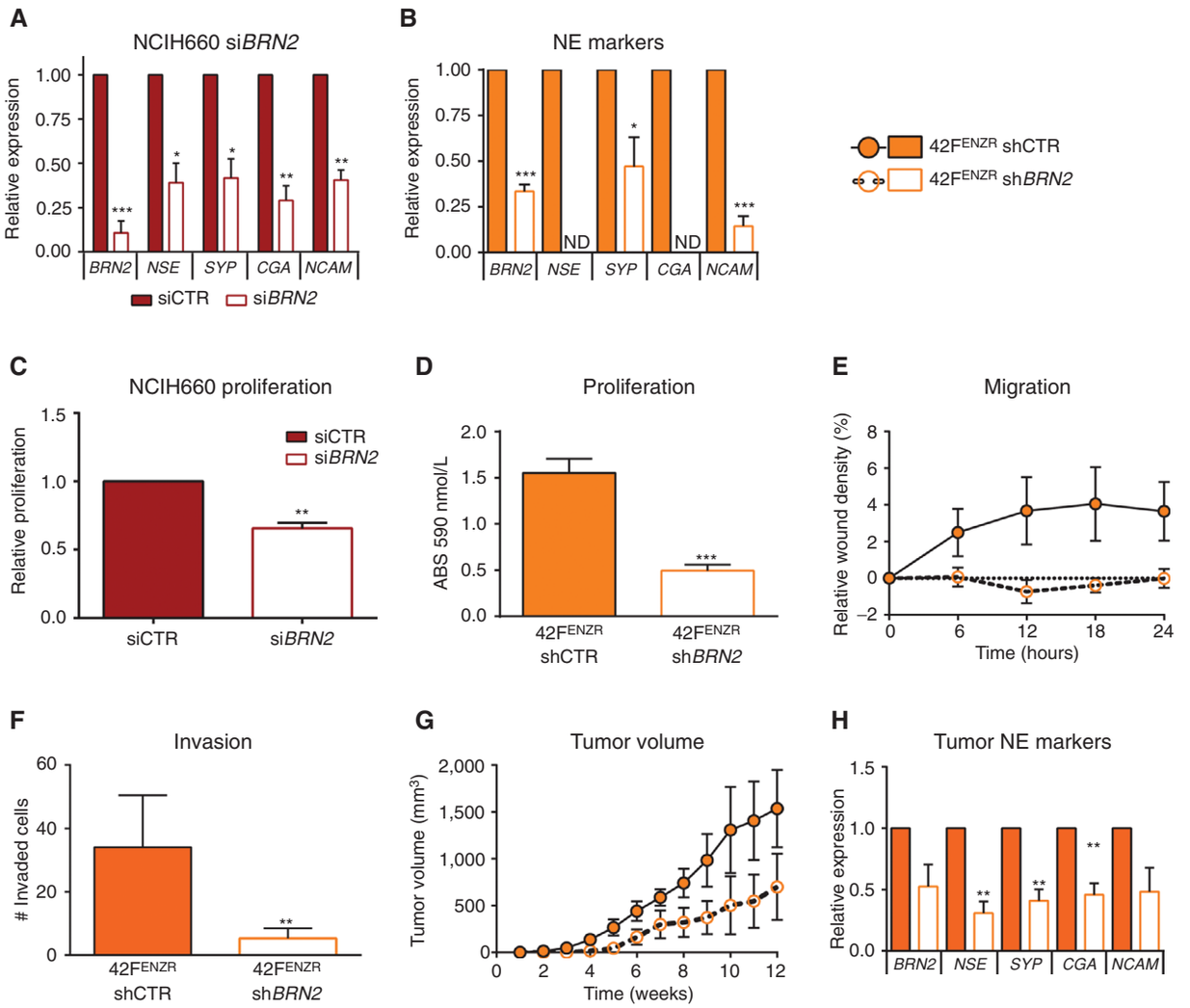

Figure 7. BRN2 is required for neuroendocrine marker expression and aggressive growth of ENZ^R cells *in vitro* and *in vivo*. **A** and **B,** Relative mRNA expression of BRN2 and NE markers in (**A**) NCIH660 cells transfected with *BRN2* siRNA (si*BRN2*) compared with control (siCTR = 1) and (**B**) 42F^{ENZR} cells with stable BRN2 knockdown (sh*BRN2*) compared with control transfected cells (shCTR =1). **C,** Relative proliferation, 72 hours after seeding in NCIH660 cells transfected with *BRN2* siRNA (si*BRN2*) compared with control (siCTR = 1). **D–F,** Relative proliferation (**D**), relative wound density in one-dimensional scratch assay (**E**) and number of cells migrated through Matrigel Boyden chamber (**F**) in 42F^{ENZR} cells with stable BRN2 knockdown (sh*BRN2*) compared with control-transfected cells (shCTR =1). **G,** Tumor volume of 42F^{ENZR} shCTR and 42F^{ENZR} sh*BRN2* xenografts grown *in vivo* ($n = 10$). **H,** Relative mRNA expression of BRN2 and NE markers in 42F^{ENZR} sh*BRN2* versus shCTR xenografts (= 1) harvested at 12 weeks after inoculation. Graph represents pooled data from 6 sh*BRN2* and 6 shCTR tumors. See also Supplementary Fig. S8. Statistical analyses were performed on pooled data from at least three independent experiments. *, $P < 0.05$; **, $P < 0.01$; ***, $P < 0.001$.

DISCUSSION

Clinical evidence suggests that the repercussion of potent AR suppression with APIs for a subset of patients with CRPC is the development of highly lethal NEPC tumors (20). Our work reveals several novel findings with implications for patients with CRPC and NEPC. First and foremost, we identify the master neural transcription factor BRN2 as a central and clinically relevant driver of NE marker expression in advanced prostate cancer. Utilizing a "non–AR-driven" *in vivo*–derived model of ENZ^R- and ENZ-treated CRPC, we identified BRN2 as a direct target suppressed by the AR that is both sufficient and required for NE differentiation in prostate cancer and mediates resistance to ENZ. Secondly, our data show for the first time the BRN2-dependent regulation of SOX2 in prostate cancer, and the importance of BRN2 over SOX2 in promoting NEPC. Lastly, our data reveal a striking overlap of AR and SOX binding motifs in the enhancer region of BRN2 that allow the AR to competitively inhibit the interaction between SOX2 and the BRN2 enhancer. These *in vitro*, *in vivo*, and human studies highlight BRN2 as a key driver of NE differentiation that may indicate progression toward a non–AR-driven or NE phenotype in patients with prostate cancer. Moreover,

Published OnlineFirst October 26, 2016; DOI: 10.1158/2159-8290.CD-15-1263

they suggest that relieving AR suppression of BRN2 could be a central mechanism driving NE differentiation, making BRN2 a strong potential therapeutic target for the treatment and/or prevention of NEPC.

BRN2 is a POU-domain transcription factor well described in developmental biology, where it plays an essential role in neural cell differentiation (32). In addition, BRN2 is highly expressed in NE small cell lung cancer (SCLC), where it acts upstream of other key regulators of neural programming (45) and is required for aggressive tumor growth (46). Complementing these reports, BRN2 was a highly expressed master neural transcription factor identified by RNA sequencing of our non–AR-driven ENZ^R cell lines, making it our top candidate for a potential driver of ENZ-induced NE differentiation in prostate cancer. Indeed, we found that BRN2 was not only sufficient to increase terminal markers of NE differentiation in CRPC but was also required for their expression in CRPC cells exposed to ENZ, in ENZ^R cell lines and in *bona fide* NEPC NCIH660 cells. Importantly, inhibiting BRN2 expression and concomitant reduction in NE markers in both ENZ^R and CRPC cells functionally led to significantly reduced proliferation, migration, and invasion, as well as decreased ENZ^R tumor growth *in vivo* and increased resistance to ENZ *in vitro*. These data mirror other reports showing the requirement for BRN2 in SCLC (46, 47) as well as in melanoma, where it is required for invasion and migration (48–50). Importantly, we have identified BRN2 as a major regulator of NE differentiation in a model of castration- and ENZ-resistant prostate cancer and in terminally differentiated NEPC cell lines.

Data from human specimens brought clinical relevance to BRN2 in aggressive prostate cancer tumors, including NEPC. RNA-sequencing data from patient cohorts showed that BRN2 was most highly expressed in clinically defined NEPC tumors compared with adenocarcinomas. Importantly, however, BRN2 was identified in CRPC specimens as well, indicating that BRN2 is not a specific marker of NEPC, but rather may indicate potential toward disease progression, especially in a setting of androgen deprivation. This was in accordance with our data showing that BRN2 is inducible in CRPC cells under the pressure of ENZ and supported our hypothesis that it is an androgen-suppressed gene. Indeed, we found BRN2 was most highly expressed in primary adenocarcinoma or CRPC tissue from patients with low levels of circulating PSA, and BRN2 expression significantly increased from progression to CRPC only in patients with low PSA levels. Publicly available data mirrored this inverse correlation between high BRN2 expression and low circulating PSA, and further underscored the association between BRN2 and the potential for NE-like disease, as it positively correlated with SYP and CGA expression.

Human data implicating AR control of BRN2 were complemented by mechanistic studies using ENZ^R cell lines, which showed that BRN2 is suppressed by the AR through ligand-dependent binding to an ARE in the enhancer region of BRN2. AR binding to this site resulted in reduced levels of not only NE markers but also SOX2, which we also found highly expressed in human NEPC. SOX2 is a well-defined transcription factor that supports the proliferation and invasiveness of prostate cancer (43, 51–53), is associated with NEPC (40), and is required for the function and maintenance of NPCs (54). Importantly, however, SOX2 can only drive a neural development program by cooperating with other master transcription factors, especially POU family members (41). In particular, BRN2 and SOX2 co-bind upstream of many genes with central roles in neural cell fate and function (42, 55). Moreover, BRN2 is a key regulator of SOX2 activity in NPCs, a function that is highly evolutionarily conserved (44, 55). Despite extensive research into this "pou-sox code" in neural development, how SOX2 is regulated in prostate cancer is largely unexplored. Our study shows that BRN2 is required for SOX2 expression in both CRPC cells treated with ENZ as well as ENZ^R cells. The regulation of SOX2 by AR may be compounded by direct enhancer binding (43) and via AR-dependent suppression of BRN2. Indeed, as we found for BRN2, SOX2 is more highly expressed in AR$^-$ than AR$^+$ prostate cancer cell lines (40) and is higher in NEPC and metastatic CRPC than in adenocarcinoma (40, 43, 56). Altogether, these data suggest that the link between SOX2 and progression to AR-independent CRPC or NEPC may be a result of increased BRN2 expression.

Our results showing BRN2-mediated regulation of SOX2 also shed light on the importance of BRN2 over SOX2 in driving NE differentiation in prostate cancer cells. Although SOX2 is present in NE tumors of not only the prostate (40) but also the lung (57, 58) and skin (59), these studies have not shown a direct requirement of SOX2 in supporting this phenotype. Our results suggest that whereas SOX2 overexpression alone in CRPC cells can marginally increase expression of CGA, NSE, SYP, and NCAM1, SOX2 requires the presence of BRN2 to significantly upregulate the expression of these NE markers. The hypothesis that BRN2 and SOX2 work together to drive a neural program in CRPC cells is further supported by our data showing direct BRN2–SOX2 protein–protein interaction at the enhancer region of neuronal genes, leading to their upregulation in ENZ^R cells, which is in accordance with previously reported ChIP-seq analysis (42). Importantly, however, although BRN2 and SOX2 can both bind upstream of each other in NPCs (42), the controlling signals as well as the consequences of these binding events remain unclear. Intriguingly, our observation that SOX2 bound to a canonical SOX motif that overlapped with the ARE in the enhancer region of BRN2 suggests that the AR may play an important role in controlling SOX protein DNA binding in prostate cancer cells. Although the consequence of this inhibition of SOX2 binding to the BRN2 enhancer in the presence of androgen remains unclear, it may be that this interaction supports the two factors coordinating to drive downstream neural gene expression.

Although multiple pathways likely converge to drive the emergence of NEPC, understanding the contribution of the AR to this disease is critical for better implementation of current API therapies and novel drug design. Together, data from our human cohorts and *in vitro* mechanistic analysis strongly implicate BRN2 as an androgen-suppressed transcription factor that plays a significant role in the progression of prostate cancer from adenocarcinoma to NEPC, making it a potentially attractive and novel therapeutic target.

Published OnlineFirst October 26, 2016; DOI: 10.1158/2159-8290.CD-15-1263

METHODS

Generation of ENZR Xenografts and Cell Lines

The detailed procedure for generation of CRPC and ENZ^R tumors and cell lines is found in Supplementary Methods as well as our previously published report (60). A schematic depicting model generation and growth of individual xenografts from which cell lines are derived is shown in Supplementary Fig. S1.

Cell Line Culture and Reagents

PC3, NCIH660, and LAPC4 cells were obtained from the ATCC in 2013. LNCaP cells were kindly provided by Dr. Leland W.K. Chung (Emory University) and authenticated in January 2013. CRPC and ENZ^R cell lines were generated from LNCaP cells (60), tested, and authenticated by whole-genome and whole-transcriptome sequencing (Illumina Genome Analyzer IIx, 2012). Cells were maintained in RPMI-1640 (LNCaP-derived and PC3) or Iscove's Modified Dulbecco's Medium (LAPC4), containing 10% FBS, 100 U/mL penicillin-G, 100 mg/mL streptomycin (all Hyclone), ±10 μmol/L ENZ (Haoyuan Chemexpress), or DMSO (Sigma-Aldrich) vehicle (for ENZ^R vs. CRPC, PC3 did not receive ENZ). Where indicated, CRPC or LAPC4 cells induced to an NE phenotype were cultured in RPMI-1640, 10% FBS, 100 U/mL penicillin-G, 100 mg/mL streptomycin, +10 μmol/L ENZ for 7 days prior to downstream analysis. Cells were seeded at a density of 10^6 cells/10 mL media and harvested after 72 hours unless otherwise noted.

Generation of BRN2 CRISPR Knockout Cells

Cells were transfected with 500-ng GeneArt Platinum Cas9 nuclease (Thermo) and 125-ng guide RNA (gRNA) using Lipofectamine CRISPRMAX (Thermo). The targeting gRNA sequence 5′-GCTGTAGTGGTTAGACGCTG-3′ was used to edit exon 1 of the POU3F1 locus. At 72 hours after transfection, cells were harvested for analysis of genome modification efficiency using the GeneArt Genomic Cleavage Detection Kit (Thermo) with the forward primer 5′-AAATCAAAGGGCGCGGCGCC-3′ and reverse primer 5′-GCCGCCGCCGTGGGACAG-3′. Ten individual clones were isolated and assessed for indels at the POU3F2 locus by Sanger sequencing.

Cell Line and Tumor Microarray and RNA Sequencing

Microarray gene expression was performed as previously described (36) using Agilent SurePrint G3 Human GE 8 × 60 K slides (Design ID 028004) and analyzed using Agilent GeneSpring 11.5.1 and Ingenuity Knowledge Base (Ingenuity Systems). Specimens were prepared for RNA sequencing using the TruSeq RNA Library Preparation Kit v2, and transcriptome sequencing (RNA-seq) was performed using Illumina HiSeq 2000 (Illumina Inc.) or HiSeq 2500 (human tumors) according to standard protocols. Sequence data mapping and processing was performed as previously described (61), except normalization was performed using reads per million. Quantification of gene expression was performed via RSEQtools using GENCODE v19 as reference gene annotation set. Expression levels (RPKM) were estimated by counting all nucleotides mapped to the gene and normalized by the total number of mapped nucleotides (per million) and the gene length (per kilobase). Sequencing of the AR ligand binding domain was performed exactly as previously described (26). To assess global differences in gene expression in microarray and RNA-sequencing data, multidimensional scaling to analyze differences between cell line gene expression data was performed using the PCoA tool in XLSTAT software (Addinsoft).

Cell Line Transfection

CRPC or ENZ^R cells were seeded at a density of 10^6 cells/10 mL complete media in 10-cm tissue culture dishes (Corning Life Sciences) 18 to 24 hours prior to transfection with siRNA, shRNA, plasmid overexpression, or DNA aptamer.

siRNA

Cells were transfected with 10 nmol/L BRN2#1 or control siRNA (Santa Cruz Biotechnology), 10 nmol/L of BRN2#2 and si*SOX2* (Life Technology) using Oligofectamine (Invitrogen), and OPTI-MEM media (Gibco). After 18 hours, cells were retransfected. After 4 hours, OPTI-MEM media were replaced with complete media, and cells were harvested after 48 hours.

shRNA

The same protocol as siRNA was used for sh*BRN2* transfections using sh*BRN2* or control shRNA (Santa Cruz Biotechnology) and successfully transfected clones were selected for and expanded in complete media containing 10 μg/mL puromycin.

Overexpression

SOX2 plasmid (1 μg; Addgene, #16353) or 8 μg BRN2 plasmid (Addgene, #19711) was transfected using Mirus T20/20 and OPTI-MEM media (Invitrogen) according to the manufacturer's instructions. After 18 to 24 hours, OPTI-MEM media were replaced with complete media ± 10 μmol/L ENZ, and cells were harvested after 7 days or at indicated time points. For 7-day experiments, CRPC cells were retransfected on day 4.

siRNA/Overexpression

Cells were plasmid transfected with Mirus T20/20 on day 1 and the following day transfected with siRNA with Oligofectamine. After 18 to 24 hours cells were retransfected with siRNA, and OPTI-MEM was replaced with complete media ±10 μmol/L ENZ and harvested 48 hours later (total 5 days).

BRN2 Aptamer

Indicated doses of BRN2–ARE aptamer were transfected into cells using Oligofectamine. After 18 hours, cells were transfected for a second time for 4 hours. This was repeated on day 4, and cells were either in OPTI-MEM or in complete media + 10 μmol/L ENZ. 42D^{ENZR} cells were transfected with the aptamer, and after 18 hours transfected a second time. Following this, they were exposed to R1881 for 48 hours, and samples were harvested. For aptamer sequence please see Supplementary Table S4.

qRT-PCR

Total RNA was extracted from cells using TRIzol reagent (Life Technology) and 2 μg was reversed transcribed using MMLV reverse transcriptase and random hexamers (Invitrogen). Real-time PCR was performed using SyberGreen ROX Master Mix (Roche Applied Science). Target gene expression was normalized to GAPDH levels in three experimental replicates per sample. For primer sequences, please see Supplementary Table S4.

Immunoprecipitation and Western Blotting

Immunoprecipitation was performed using the ImmunoCruz IP/WB Optima B System (Santa Cruz Biotechnology) based on the manufacturer's guideline. Dilution (1/50) of primary antibody was used for immunoprecipitation. Total proteins were extracted from adherent cells grown *in vitro* using RIPA lysis buffer. Forty micrograms of protein was resolved by SDS-PAGE, and the following antibodies were used for Western blot: AR, PSA, BRN2, SYP (Cell Signaling Technology), NSE (Dako), SOX2 (Millipore), and CGA and vinculin (Sigma-Aldrich). Blots were incubated overnight at 4°C with designated primary antibodies at 1:1,000 dilution, unless noted

Published OnlineFirst October 26, 2016; DOI: 10.1158/2159-8290.CD-15-1263

otherwise. Proteins were visualized using the Odyssey system (Li-Cor Biosciences).

Luciferase Assay

CRPC and ENZ^R cells were plated in 6-well plates (2×10^4 cells/cm^2) and transfected with a BRN2 luciferase reporter (courtesy of Dr. Goding, Ludwig Institute for Cancer Research, Oxford, UK; ref. 62) or Renilla (Promega) using Lipofectin (Invitrogen). The total plasmid DNA used was normalized to 0.5 μg per well by the addition of Renilla. At 24 hours after transfection, cells were incubated with or without 10 nmol/L R1881 for 24 hours, and luciferase activities were measured using a Dual-Luciferase Reporter Assay System (Promega) and a Tecan Infinite 200 PRO microplate luminometer (Tecan). BRN2 luciferase activities were corrected by the corresponding Renilla luciferase activities. Results are expressed in arbitrary light units.

Flow Cytometry

Cells were harvested using citric saline for 10 minutes at room temperature and washed in RPMI+10% FBS. Before antibody addition, cells were incubated with human Fc receptor Binding Inhibitor (eBioscience) for 20 minutes on ice. Flow cytometry staining was performed using anti-human NCAM1 followed by staining with viability marker 7-aminoactinomycin D (7-AAD; both eBioscience, per instructions) and fixation in 2% paraformaldehyde (PFA). Data were acquired (minimum 30K events) on a Canto II (BD Biosciences) and analyzed with FlowJo (TreeStar).

Proliferation Assay

The WST-1 (Promega) assay was used to assess cell growth according to the manufacturer's protocol. One thousand cells were seeded in 96-well plates in complete media, and absorbance at 450 nm was measured after 72 hours.

Migration Assay

Cell migration was assessed in a wound-healing assay. Cells were plated on Essen ImageLock 96-well plates (Essen Instruments) and incubated for 2 hours with mitomycin (5 μg/mL) prior to wound scratching with a wound scratcher (Essen Instruments) 24 hours after plating. Wound confluence was monitored with the IncuCyte Zoom Live-Cell Imaging System and software (Essen Instruments). Wound closure was measured every 6 hours for 24 hours by comparing the mean relative wound density of three replicates.

Invasion Assay

Invasion was assessed by the invasion of 2.5×10^4 cells through BioCoat Matrigel-coated Transwell inserts with 8-μm pore size (BD Biosciences). After 24 hours, the Transwell insert was removed and fixed for 10 minutes in 100% methanol (Sigma-Aldrich) at −20°C and mounted on glass cover slips with Vectashield Mounting Media with DAPI (Vector Laboratories). Filters were imaged using Zeiss Axioplan II microscope (Zeiss) and cells invaded in membrane were quantified.

ChIP and Sequential ChIP (Re-ChIP)

Cells treated with or without 1 nmol/L R1881 for 24 hours were cross-linked with PFA (Sigma-Aldrich) and sonicated to shear DNA. ChIP assay was performed using the ChIP Assay Kit (Agarose Beads) according to the manufacturer's protocol (Millipore) and antibodies against AR (N20; Santa Cruz Biotechnology) and SOX2 (Millipore). Negative control primers were designed for the regions approximately 1600 bp upstream and 1800 bp downstream of the ARE 8733 bp upstream of BRN2 TSS using Primer Express 3 (Thermo Fisher). Re-ChIP was performed via a Re-ChIP-IT kit (Active Motif Inc.), based on the manufacturer's protocol using antibodies against BRN2 (Cell Signaling Technology) and SOX2 (Millipore). IgG was used as a negative control for antibodies, and negative control primers for each binding site were designed as listed in Supplemental Experimental Procedures. Using Primer Express 3 (Thermo Fisher), primers were designed around BRN2/SOX2 consensus binding elements approximately 7,500 bp upstream of NES start codon and 35,000 bp downstream of RFX4 start codon. Negative control primers were approximately 5,400 bp upstream of NES start codon and 38,000 bp downstream of RFX4 start codon. For primer sequences please see Supplementary Table S4.

Xenograft Studies

sh*BRN2* and shCTR ENZ^R tumors were grown and monitored *in vivo* in castrated male athymic mice (Harlan Sprague-Dawley) under pressure of daily oral 10 mg/kg ENZ. Tumors were monitored for growth, and blood was drawn for PSA screening weekly as previously described (60). When tumors reached 1,000 mm^3 or greater than 10% animal body weight, tumors were harvested and processed for RNA analysis by qRT-PCR. All animal procedures were conducted according to the guidelines of the Canadian Council on Animal Care.

Human Prostate Cancer Specimens for RNA-seq and Immunohistochemistry

RNA-seq was performed as above on samples from the Weill Cornell College of Medicine: Beltran 2016 (phs000909.v.p1, cBioportal; ref. 33) = 68 adenocarcinoma, 34 CRPC-Adeno, and 15 CRPC-NE; Beltran 2011 (phs000310 .v.p1, cBioportal) = 30 Adeno and 7 NEPC (11). Tumors were classified by the following criteria based on histomorphology (11, 33): Adeno, usual prostate adenocarcinoma without neuroendocrine differentiation (from radical prostatectomy); CRPC, tumor obtained from CRPC adenocarcinoma metastasis without neuroendocrine differentiation; and NEPC, either of the following categories, adenocarcinoma with >20%, neuroendocrine differentiation, small cell carcinoma, large cell neuroendocrine carcinoma, or mixed small cell carcinoma—adenocarcinoma. For IHC, prostate cancer specimens were obtained from the Vancouver Prostate Centre Tissue Bank and were classified as above (Adeno, n = 93; CRPC, n = 30; NEPC, n = 11). Tissue microarrays of duplicate 1-mm cores were constructed manually (Beecher Instruments). Samples were from radical prostatectomy or transurethral resection of prostate. Immunohistochemical staining was conducted as previously described (36) using the Ventana DiscoverXT Autostainer (Ventana Medical System) with enzyme labeled biotin streptavidin system and a solvent-resistant DAB Map Kit by using 1 of 150 concentration of BRN2 (Abcam) and 1 of 25 concentrations of CGA and AR (Sigma) antibodies. Specimens were graded from 0 to +3 intensity by visual scoring, representing negative-heavy staining. Automated quantitative image analysis was conducted using pro-plus image software. Scoring was conducted at 200× magnification.

Statistical Analysis and Data Representation

Pearson correlations (95% confidence interval) were performed using GraphPad Prism (GraphPad Software) for IHC scoring and BRN2 versus serum PSA. In bar graphs, unpaired, two-tailed, Student t tests were performed to analyze statistical significance between groups using GraphPad Prism (GraphPad Software).

Published OnlineFirst October 26, 2016; DOI: 10.1158/2159-8290.CD-15-1263

Significance is indicated as follows: *, $P < 0.05$; **, $P < 0.01$; ***, $P < 0.001$; ****, $P < 0.0001$. Graphs show pooled data with error bars representing SEM obtained from at least three independent experiments.

Disclosure of Potential Conflicts of Interest

C.C. Collins is a consultant/advisory board member for Accuragen. No potential conflicts of interest were disclosed by the authors.

Authors' Contributions

Conception and design: J.L. Bishop, D. Thaper, S. Vahid, M.E. Gleave, A. Zoubeidi

Development of methodology: J.L. Bishop, D. Thaper, S. Vahid, A. Davies, K.M. Nip, A. Zoubeidi

Acquisition of data (provided animals, acquired and managed patients, provided facilities, etc.): J.L. Bishop, D. Thaper, S. Vahid, H. Kuruma, A. Angeles, F. Johnson, M.E. Gleave, M.A. Rubin, Y. Wang

Analysis and interpretation of data (e.g., statistical analysis, biostatistics, computational analysis): J.L. Bishop, D. Thaper, S. Vahid, K. Ketola, H. Kuruma, R. Jama, K.M. Nip, A.W. Wyatt, C.C. Collins, Y. Wang, H. Beltran, A. Zoubeidi

Writing, review, and/or revision of the manuscript: J.L. Bishop, D. Thaper, S. Vahid, A. Davies, K. Ketola, R. Jama, C.C. Collins, H. Beltran, A. Zoubeidi

Administrative, technical, or material support (i.e., reporting or organizing data, constructing databases): J.L. Bishop, R. Jama, K.M. Nip, A. Angeles, D. Lin, C.C. Collins

Study supervision: J.L. Bishop, A. Zoubeidi

Other (pathology): L. Fazli

Acknowledgments

Tissue procurement and tissue microarray construction at the Vancouver Prostate Centre were supported by the Terry Fox New Frontiers Program Project Grant. We thank Dr. Goding (Ludwig Institute for Cancer Research, Oxford, UK) for providing the BRN2 luciferase plasmid and Mary Bowden and Darrell Trendall for technical support in animal studies.

Grant Support

This work is supported by the Prostate Cancer Foundation USA and Prostate Cancer Canada, and proudly funded by the Movember Foundation (T2013-01). J.L. Bishop was supported by the Prostate Cancer Foundation Young Investigator Award and the Urology Care Foundation. K. Ketola was supported by the U.S. Department of Defense (PC121341). D. Thaper and A. Davies were supported by a Canadian Institute of Health Research scholarship.

The costs of publication of this article were defrayed in part by the payment of page charges. This article must therefore be hereby marked *advertisement* in accordance with 18 U.S.C. Section 1734 solely to indicate this fact.

Received October 22, 2015; revised October 20, 2016; accepted October 21, 2016; published OnlineFirst October 26, 2016.

REFERENCES

1. Ferraldeschi R, Welti J, Luo J, Attard G, de Bono JS. Targeting the androgen receptor pathway in castration-resistant prostate cancer: progresses and prospects. Oncogene 2015;34:1745–57.
2. Scher HI, Fizazi K, Saad F, Taplin ME, Sternberg CN, Miller K, et al. Increased survival with enzalutamide in prostate cancer after chemotherapy. N Engl J Med 2012;367:1187–97.
3. Beltran H, Tomlins S, Aparicio A, Arora V, Rickman D, Ayala G, et al. Aggressive variants of castration-resistant prostate cancer. Clin Cancer Res 2014;20:2846–50.
4. Small EJ, Huang J, Youngren J, Sokolov A, Aggarwal RR, Thomas G, et al. Characterization of neuroendocrine prostate cancer (NEPC) in patients with metastatic castration resistant prostate cancer (mCRPC) resistant to abiraterone (Abi) or enzalutamide (Enz): Preliminary results from the SU2C/PCF/AACR West Coast Prostate Cancer Dream Team (WCDT). ASCO Annual Meeting 2015;33 (abstract 5003).
5. Epstein JI, Amin MB, Beltran H, Lotan TL, Mosquera JM, Reuter VE, et al. Proposed morphologic classification of prostate cancer with neuroendocrine differentiation. Am J Surg Pathol 2014;38:756–67.
6. Aparicio A, Logothetis CJ, Maity SN. Understanding the lethal variant of prostate cancer: power of examining extremes. Cancer Discov 2011;1:466–8.
7. Alanee S, Moore A, Nutt M, Holland B, Dynda D, El-Zawahry A, et al. Contemporary incidence and mortality rates of neuroendocrine prostate cancer. Anticancer Res 2015;35:4145–50.
8. Tan HL, Sood A, Rahimi HA, Wang W, Gupta N, Hicks J, et al. Rb loss is characteristic of prostatic small cell neuroendocrine carcinoma. Clin Cancer Res 2014;20:890–903.
9. Tzelepi V, Zhang J, Lu JF, Kleb B, Wu G, Wan X, et al. Modeling a lethal prostate cancer variant with small-cell carcinoma features. Clin Cancer Res 2012;18:666–77.
10. Chen H, Sun Y, Wu C, Magyar CE, Li X, Cheng L, et al. Pathogenesis of prostatic small cell carcinoma involves the inactivation of the P53 pathway. Endocr Relat Cancer 2012;19:321–31.
11. Beltran H, Rickman DS, Park K, Chae SS, Sboner A, MacDonald TY, et al. Molecular characterization of neuroendocrine prostate cancer and identification of new drug targets. Cancer Discov 2011;1:487–95.
12. Akamatsu S, Wyatt AW, Lin D, Lysakowski S, Zhang F, Kim S, et al. The placental gene PEG10 promotes progression of neuroendocrine prostate cancer. Cell Rep 2015;12:922–36.
13. Lapuk AV, Wu C, Wyatt AW, McPherson A, McConeghy BJ, Brahmbhatt S, et al. From sequence to molecular pathology, and a mechanism driving the neuroendocrine phenotype in prostate cancer. J Pathol 2012;227:286–97.
14. Zhang X, Coleman IM, Brown LG, True LD, Kollath L, Lucas JM, et al. SRRM4 expression and the loss of REST activity may promote the emergence of the neuroendocrine phenotype in Castration-Resistant Prostate Cancer. Clin Cancer Res 2015;21:4698–708.
15. Svensson C, Ceder J, Iglesias-Gato D, Chuan YC, Pang ST, Bjartell A, et al. REST mediates androgen receptor actions on gene repression and predicts early recurrence of prostate cancer. Nucleic Acids Res 2014;42:999–1015.
16. Wee ZN, Li Z, Lee PL, Lee ST, Lim YP, Yu Q. EZH2-mediated inactivation of IFN-gamma-JAK-STAT1 signaling is an effective therapeutic target in MYC-driven prostate cancer. Cell Rep 2014;8:204–16.
17. Li Y, Donmez N, Sahinalp C, Xie N, Wang Y, Xue H, et al. SRRM4 drives neuroendocrine transdifferentiation of prostate adenocarcinoma under androgen receptor pathway inhibition. Eur Urol 2016 May 11. pii: S0302-2838(16)30138-5. doi: 10.1016/j.eururo.2016.04.028. [Epub ahead of print].
18. Abrahamsson PA. Neuroendocrine differentiation and hormone-refractory prostate cancer. Prostate Suppl 1996;6:3–8.
19. Burchardt T, Burchardt M, Chen MW, Cao Y, de la Taille A, Shabsigh A, et al. Transdifferentiation of prostate cancer cells to a neuroendocrine cell phenotype in vitro and in vivo. J Urol 1999;162:1800–5.
20. Hu CD, Choo R, Huang J. Neuroendocrine differentiation in prostate cancer: a mechanism of radioresistance and treatment failure. Front Oncol 2015;5:90.
21. Kani K, Malihi PD, Jiang Y, Wang H, Wang Y, Ruderman DL, et al. Anterior gradient 2 (AGR2): blood-based biomarker elevated in metastatic prostate cancer associated with the neuroendocrine phenotype. Prostate 2013;73:306–15.

Published OnlineFirst October 26, 2016; DOI: 10.1158/2159-8290.CD-15-1263

22. Rapa I, Volante M, Migliore C, Farsetti A, Berruti A, Vittorio Scagliotti G, et al. Human ASH-1 promotes neuroendocrine differentiation in androgen deprivation conditions and interferes with androgen responsiveness in prostate cancer cells. Prostate 2013;73:1241–9.
23. Arora VK, Schenkein E, Murali R, Subudhi SK, Wongvipat J, Balbas MD, et al. Glucocorticoid receptor confers resistance to antiandrogens by bypassing androgen receptor blockade. Cell 2013;155:1309–22.
24. Asangani IA, Dommeti VL, Wang X, Malik R, Cieslik M, Yang R, et al. Therapeutic targeting of BET bromodomain proteins in castration-resistant prostate cancer. Nature 2014;510:278–82.
25. Balbas MD, Evans MJ, Hosfield DJ, Wongvipat J, Arora VK, Watson PA, et al. Overcoming mutation-based resistance to antiandrogens with rational drug design. eLife 2013;2:e00499.
26. Azad AA, Volik SV, Wyatt AW, Haegert A, Le Bihan S, Bell RH, et al. Androgen receptor gene aberrations in circulating cell-free DNA: biomarkers of therapeutic resistance in castration-resistant prostate cancer. Clin Cancer Res 2015;21:2315–24.
27. Joseph JD, Lu N, Qian J, Sensintaffar J, Shao G, Brigham D, et al. A clinically relevant androgen receptor mutation confers resistance to second-generation antiandrogens enzalutamide and ARN-509. Cancer Discov 2013;3:1020–9.
28. Korpal M, Korn JM, Gao X, Rakiec DP, Ruddy DA, Doshi S, et al. An F876L mutation in androgen receptor confers genetic and phenotypic resistance to MDV3100 (enzalutamide). Cancer Discov 2013;3:1030–43.
29. Lee JK, Phillips JW, Smith BA, Park JW, Stoyanova T, McCaffrey EF, et al. N-Myc drives neuroendocrine prostate cancer initiated from human prostate epithelial cells. Cancer Cell 2016;29:536–47.
30. Hubbard GK, Mutton LN, Khalili M, McMullin RP, Hicks JL, Bianchi-Frias D, et al. Combined MYC activation and Pten loss are sufficient to create genomic instability and lethal metastatic prostate cancer. Cancer Res 2016;76:283–92.
31. Shappell SB, Thomas GV, Roberts RL, Herbert R, Ittmann MM, Rubin MA, et al. Prostate pathology of genetically engineered mice: definitions and classification. The consensus report from the Bar Harbor meeting of the Mouse Models of Human Cancer Consortium Prostate Pathology Committee. Cancer Res 2004;64:2270–305.
32. Dominguez MH, Ayoub AE, Rakic P. POU-III transcription factors (Brn1, Brn2, and Oct6) influence neurogenesis, molecular identity, and migratory destination of upper-layer cells of the cerebral cortex. Cereb Cortex 2013;23:2632–43.
33. Beltran H, Prandi D, Mosquera JM, Benelli M, Puca L, Cyrta J, et al. Divergent clonal evolution of castration-resistant neuroendocrine prostate cancer. Nat Med 2016;22:298–305.
34. Kaplan-Lefko PJ, Chen TM, Ittmann MM, Barrios RJ, Ayala GE, Huss WJ, et al. Pathobiology of autochthonous prostate cancer in a pre-clinical transgenic mouse model. Prostate 2003;55:219–37.
35. Tarhini AA, Edington H, Butterfield LH, Lin Y, Shuai Y, Tawbi H, et al. Immune monitoring of the circulation and the tumor microenvironment in patients with regionally advanced melanoma receiving neoadjuvant ipilimumab. PLoS One 2014;9:e87705.
36. Lin D, Wyatt AW, Xue H, Wang Y, Dong X, Haegert A, et al. High fidelity patient-derived xenografts for accelerating prostate cancer discovery and drug development. Cancer Res 2014;74:1272–83.
37. Grasso CS, Wu YM, Robinson DR, Cao X, Dhanasekaran SM, Khan AP, et al. The mutational landscape of lethal castration-resistant prostate cancer. Nature 2012;487:239–43.
38. Taylor BS, Schultz N, Hieronymus H, Gopalan A, Xiao Y, Carver BS, et al. Integrative genomic profiling of human prostate cancer. Cancer Cell 2010;18:11–22.
39. Barton BE, Murphy TF, Shu P, Huang HF, Meyenhofer M, Barton A. Novel single-stranded oligonucleotides that inhibit signal transducer and activator of transcription 3 induce apoptosis in vitro and in vivo in prostate cancer cell lines. Mol Cancer Ther 2004;3:1183–91.
40. Yu X, Cates JM, Morrissey C, You C, Grabowska MM, Zhang J, et al. SOX2 expression in the developing, adult, as well as, diseased prostate. Prostate Cancer Prostatic Dis 2014;17:301–9.
41. Dailey L, Basilico C. Coevolution of HMG domains and homeodomains and the generation of transcriptional regulation by Sox/POU complexes. J Cell Physiol 2001;186:315–28.
42. Lodato MA, Ng CW, Wamstad JA, Cheng AW, Thai KK, Fraenkel E, et al. SOX2 co-occupies distal enhancer elements with distinct POU factors in ESCs and NPCs to specify cell state. PLoS Genet 2013;9:e1003288.
43. Kregel S, Kiriluk KJ, Rosen AM, Cai Y, Reyes EE, Otto KB, et al. Sox2 is an androgen receptor-repressed gene that promotes castration-resistant prostate cancer. PLoS One 2013;8:e53701.
44. Iwafuchi-Doi M, Yoshida Y, Onichtchouk D, Leichsenring M, Driever W, Takemoto T, et al. The Pou5f1/Pou3f-dependent but SoxB-independent regulation of conserved enhancer N2 initiates Sox2 expression during epiblast to neural plate stages in vertebrates. Dev Biol 2011;352:354–66.
45. Sakaeda M, Sato H, Ishii J, Miyata C, Kamma H, Shishido-Hara Y, et al. Neural lineage-specific homeoprotein BRN2 is directly involved in TTF1 expression in small-cell lung cancer. Lab Invest 2013;93:408–21.
46. Ishii J, Sato H, Sakaeda M, Shishido-Hara Y, Hiramatsu C, Kamma H, et al. POU domain transcription factor BRN2 is crucial for expression of ASCL1, ND1 and neuroendocrine marker molecules and cell growth in small cell lung cancer. Pathol Int 2013;63:158–68.
47. Endo T, Yazawa T, Shishido-Hara Y, Fujiwara M, Shimoyamada H, Ishii J, et al. Expression of developing neural transcription factors in lung carcinoid tumors. Pathol Int 2014;64:365–74.
48. Berlin I, Denat L, Steunou AL, Puig I, Champeval D, Colombo S, et al. Phosphorylation of BRN2 modulates its interaction with the Pax3 promoter to control melanocyte migration and proliferation. Mol Cell Biol 2012;32:1237–47.
49. Boyle GM, Woods SL, Bonazzi VF, Stark MS, Hacker E, Aoude LG, et al. Melanoma cell invasiveness is regulated by miR-211 suppression of the BRN2 transcription factor. Pigment Cell Melanoma Res 2011;24:525–37.
50. Pinner S, Jordan P, Sharrock K, Bazley L, Collinson L, Marais R, et al. Intravital imaging reveals transient changes in pigment production and Brn2 expression during metastatic melanoma dissemination. Cancer Res 2009;69:7969–77.
51. Bae KM, Su Z, Frye C, McClellan S, Allan RW, Andrejewski JT, et al. Expression of pluripotent stem cell reprogramming factors by prostate tumor initiating cells. J Urol 2010;183:2045–53.
52. Jia X, Li X, Xu Y, Zhang S, Mou W, Liu Y, et al. SOX2 promotes tumorigenesis and increases the anti-apoptotic property of human prostate cancer cell. J Mol Cell Biol 2011;3:230–8.
53. Lin F, Lin P, Zhao D, Chen Y, Xiao L, Qin W, et al. Sox2 targets cyclinE, p27 and survivin to regulate androgen-independent human prostate cancer cell proliferation and apoptosis. Cell Prolif 2012;45:207–16.
54. Graham V, Khudyakov J, Ellis P, Pevny L. SOX2 functions to maintain neural progenitor identity. Neuron 2003;39:749–65.
55. Catena R, Tiveron C, Ronchi A, Porta S, Ferri A, Tatangelo L, et al. Conserved POU binding DNA sites in the Sox2 upstream enhancer regulate gene expression in embryonic and neural stem cells. J Biol Chem 2004;279:41846–57.
56. Ugolkov AV, Eisengart LJ, Luan C, Yang XJ. Expression analysis of putative stem cell markers in human benign and malignant prostate. Prostate 2011;71:18–25.
57. Sholl LM, Long KB, Hornick JL. Sox2 expression in pulmonary non-small cell and neuroendocrine carcinomas. Appl Immunohistochem Mol Morphol 2010;18:55–61.
58. Morise M, Hishida T, Takahashi A, Yoshida J, Ohe Y, Nagai K, et al. Clinicopathological significance of cancer stem-like cell markers in

Published OnlineFirst October 26, 2016; DOI: 10.1158/2159-8290.CD-15-1263

high-grade neuroendocrine carcinoma of the lung. J Cancer Res Clin Oncol 2015;141:2121–30.
59. Laga AC, Lai CY, Zhan Q, Huang SJ, Velazquez EF, Yang Q, et al. Expression of the embryonic stem cell transcription factor SOX2 in human skin: relevance to melanocyte and Merkel cell biology. Am J Pathol 2010;176:903–13.
60. Kuruma H, Matsumoto H, Shiota M, Bishop J, Lamoureux F, Thomas C, et al. A novel antiandrogen, Compound 30, suppresses castration-resistant and MDV3100-resistant prostate cancer growth in vitro and in vivo. Mol Cancer Ther 2013;12:567–76.
61. Wyatt AW, Mo F, Wang K, McConeghy B, Brahmbhatt S, Jong L, et al. Heterogeneity in the inter-tumor transcriptome of high risk prostate cancer. Genome Biol 2014;15:426.
62. Goodall J, Wellbrock C, Dexter TJ, Roberts K, Marais R, Goding CR. The Brn-2 transcription factor links activated BRAF to melanoma proliferation. Mol Cell Biol 2004;24:2923–31.

AACR American Association for Cancer Research

CANCER DISCOVERY

The Master Neural Transcription Factor BRN2 Is an Androgen Receptor–Suppressed Driver of Neuroendocrine Differentiation in Prostate Cancer

Jennifer L. Bishop, Daksh Thaper, Sepideh Vahid, et al.

Cancer Discov 2017;7:54-71. Published OnlineFirst October 26, 2016.